SCIENCE

The Apollo 16 Lunar Samples

The Apollo 16 Lunar Samples: Petrographic and Chemical Description

Apollo 16 Preliminary Examination Team

Introduction

More than four-fifths of the surface of the moon consists of a profoundly cratered, irregular surface designated terra or highlands by analogy with the terrestrial continents. These terra regions have much higher albedos than the physiographically lower and much smoother mare regions. The difference in albedo can now be ascribed to a fundamental difference in the chemical and mineralogical character of these two regions. Lunar samples from landing sites in the mare regions and high-resolution photographs taken from lunar orbit have shown that the lunar maria are underlain by extensive lava flows. Isotopic dating of samples from four mare regions (1) indicates that mare volcanism covered a time span of 600 million years beginning about 3.7 billion years ago. The intensely cratered character of the terra regions is due to both the greater antiquity of these parts of the moon and the higher flux of incoming objects that hit the moon during its very early history (2). In contrast with the mare region, the origin of the underlying material of the terra is not easily inferred from physiographic criteria. The surface manifestations of early plutonic or extrusive igneous activity—if indeed they ever existed—were erased from the terra regions by the intense early bombardment of the lunar surface. There are some portions of the highlands that may be exceptions to this generalization, in particular, large craters such as Ptolemaeus, Hipparchus, Albategnius, and Alphonsus. The regions bounded by these craters are much smoother than the typical densely cratered highlands. It is generally assumed that these regions are physiographic lows that have been filled with younger material by some poorly understood mechanism. On the basis of detailed studies of the physiographic and albedo characteristics of the basin material, it has been suggested (3) that

Fig. 1. Metric camera picture of the region around the Apollo 16 landing site, at 9°S, 15.5°E (white cross). The inset shows the approximate location of this region on the front face of the moon. The region receives its name from the very old crater Descartes centered around the scale bar in the lower portion of the photograph.

50 km

Location of Descartes
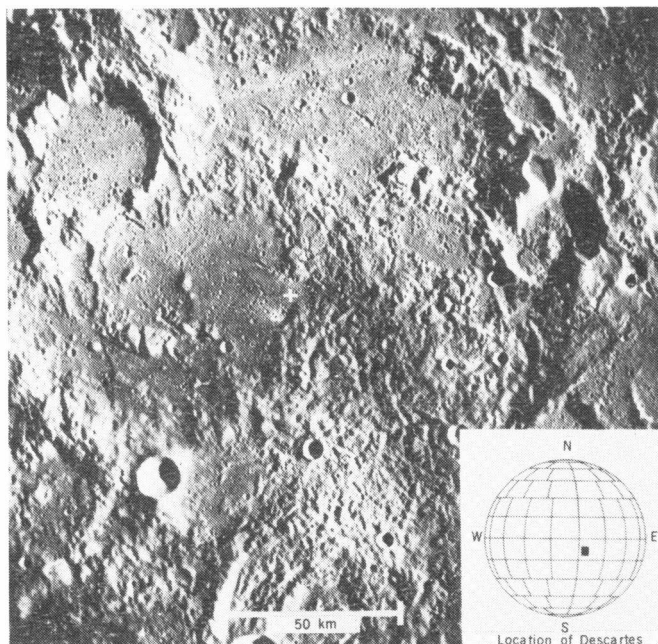
the filling of the highland basins was a result of volcanic processes similar to those which filled the large mare basins. Some highland basin areas also contain hilly, hummocky regions that bear no relation to large crater rims or crater ejecta. Theses regions have been interpreted as extrusive igneous features formed by viscous, silicic, igneous liquids (3).

The elucidation of the origin of both the filled basins and the hilly volcanic regions was the major objective of the Apollo 16 mission. Both types of landforms are remarkably common in the eastern equatorial portion of the southern highlands, facing the earth (Fig. 1). Basin-filling deposits, designated Cayley formation (4), and irregular, hilly topography, designated Descartes formation (4), occur there in close proximity.

The analysis of high-resolution photographs obtained during the Apollo 14 mission showed that a relatively smooth region 60 kilometers north of the old crater Descartes could provide a landing point with access to both landform types (8°59′29″S, 15°30′52″E). In addition, two very young, bright-rayed

craters were relatively accessible from this landing point. The age and mode of formation of these craters is of great interest, but much more important is the fact that the ejecta from these craters provides samples from material that is well below the regolith or gardened surface.

The Apollo 16 lunar module (LM) spacecraft landed successfully within less than 100 meters of the planned landing point. Three traverses extending over a region approximately 8.8 km long and 2 km wide were accomplished. Rock and soil samples were collected from ten different stations within this region. These samples include several specimens from boulders ranging to several tens of meters in size. At five of the sampling stations, rocks that are unambiguously ejecta from nearby craters were obtained. These ejecta blocks and associated soil were sampled in particular detail in order that a more detailed study could be made of the interaction of the lunar surface with both solar and galactic particles (5). In this article we summarize the chemical and petrographic characteristics of

a representative suite of the Apollo 16 rock and soil specimens. At the present time no clear-cut correlation of any of the observed characteristics with position in the site has been observed. This generalization is based on a detailed examination of only a portion of the returned samples.

Chemical Characteristics

The chemical characteristics of the Apollo 16 rocks are relatively simple and straightforward. The dominant chemical feature is the high abundance of aluminum and calcium. In a number of rocks, the absolute and relative abundances of these elements approach those of pure calcic plagioclase to a very good first approximation. The aluminum content of the rocks is directly correlated with the abundance of plagioclase, which dominates most of the rocks. Except for silicon, most of the rock-forming elements are either strongly concentrated in or excluded from plagioclase. Thus, the abundance of virtually all elements except silicon is strongly correlated with the Al_2O_3 content in the Apollo 16 rocks. The concentrations of all the major elements and several trace elements for 12 rock samples and 11 soil samples are summarized in Tables 1 and 2, respectively. The correlation with the Al_2O_3 abundance for CaO, MgO, FeO, TiO_2, and K_2O is illustrated in Figs. 2 and 3. The data in these figures show that three groups can be defined from the Al_2O_3 content alone. The first group approach pure plagioclase in composition, and they are designated here as cataclastic anorthosites. The second group—consisting of several complex breccias, one crystalline rock, and all soil samples— have Al_2O_3 contents between 26 and 29 percent. The third group have less than 26 percent Al_2O_3 and consist of rocks that are of metamorphosed igneous origin. They can be subdivided into one group having around 18 percent Al_2O_3, wit h bulk compositions similar to those of the KREEP basalts found at the Apollo 12, Apollo 14, and Apollo 15 sites (6), along with a second, more aluminum-rich group with no well-defined counterpart at other sites. The KREEP basalt type (samples 62235 and 60315) is the only rock composition from the Apollo 16 site whose major elemental abundances correspond to those of liquids known to have been produced by partial melting of the lunar or terrestrial interior.

The rather narrow range of soil compositions found at this site is remarkable when compared to those from other sites. In spite of the small range of compositions, all elements in the soils (with the possible exception of strontium and nickel) form well-defined correlations with each other. The simplicity of these correlations suggests that two end members or components prevail in these soils. They are a feldspar-rich material, perhaps similar to sample 67075, and the more ferromagnesium-rich KREEP basalt. Both the relatively low TiO_2 abundance and

Table 1. X-ray fluorescence analyses of Apollo 16 rocks. Abbreviations used: Sta., station; meta, metamorphic; ign., igneous; brec., breccia; anorth., anorthosite; %, percentage by weight; ppm, parts per million; N.D., not detected.

Component		Location, rock type, and sample number											
		Crystalline rocks						Breccias and cataclastic rocks					
		LM site meta. (III) 60315,3	Sta. 2 meta. (III) 62235,4	LM site meta. (III) 60335,1	Sta. 1 meta. (III) 61156,2	Sta. 6 meta. (III) 66095,5	Sta. 8 ign. (III) 68415,6	Sta. 1 brec. matrix (I) 61295,5	Sta. 8 brec. matrix (IV) 68815,9	Sta. 11 crushed anorth. (II) 67955,8	Sta. 13 brec. clast (II, IV) 63335,1	Sta. 1 crushed anorth. (II) 61016,3	Sta. 11 crushed anorth. (II) 67075,4
SiO_2	(%)	45.61	47.04	46.19	44.65	44.47	45.40	45.19	45.10	45.01	45.20	44.15	44.80
TiO_2	(%)	1.27	1.21	0.58	0.64	0.71	0.32	0.56	0.49	0.27	0.42	0.20	0.09
Al_2O_3	(%)	17.18	18.69	25.27	22.94	23.55	28.63	28.29	27.15	27.68	30.86	33.19	31.54
FeO	(%)	10.53	9.45	4.51	7.75	7.16	4.25	4.52	4.75	3.84	3.23	1.40	3.41
MnO	(%)	0.12	0.11	0.07	0.12	0.08	0.06	0.06	0.06	0.05	0.04	0.02	0.06
MgO	(%)	13.15	10.14	8.14	9.60	8.75	4.38	4.72	5.88	7.69	2.81	2.51	2.42
CaO	(%)	10.41	11.52	14.43	13.34	13.69	16.39	16.16	15.45	15.54	17.25	18.30	18.09
Na_2O	(%)	0.56	0.48	0.52	0.39	0.42	0.41	0.45	0.42	0.40	0.57	0.34	0.26
K_2O	(%)	0.35	0.34	0.23	0.11	0.15	0.06	0.09	0.14	0.05	0.05	0.02	0.01
P_2O_5	(%)	0.45	0.41	0.19	0.22	0.24	0.07	0.10	0.18	0.03	0.03	0.05	0.00
S	(%)	0.14	0.11	0.07	0.12	0.12	0.04	0.06	0.06	0.01	0.03	0.01	0.01
Sum		99.77	99.50	100.20	99.88	99.34	100.01	100.20	99.68	100.57	100.49	100.19	100.69
Sr	(ppm)	156	165	162	153	159	185	187	175	170	225	179	144
Rb	(ppm)	9.8	9.3	6.4	2.5	3.9	2.1	2.3	3.4	0.6	1.2	0.7	0.8
Y	(ppm)	142	193	62	64	72	23	33	61	16	11	11	2.5
Th	(ppm)	7.2	10.5	3.2	3.8	2.7	2.2	1.0	3.7	1.9	1.4	1.7	N.D.
Zr	(ppm)	640	851	281	293	322	98	143	266	59	41	48	2.7
Nb	(ppm)	37	49	16	17	18	5.6	8.6	16	4.0	3.1	2.4	N.D.
Ni	(ppm)	191	248	77	184	258	49	114	206	108	26	39	N.D.
Cr	(ppm)	1460	1370	900	960	1010	710	570	690	750	340	200	420
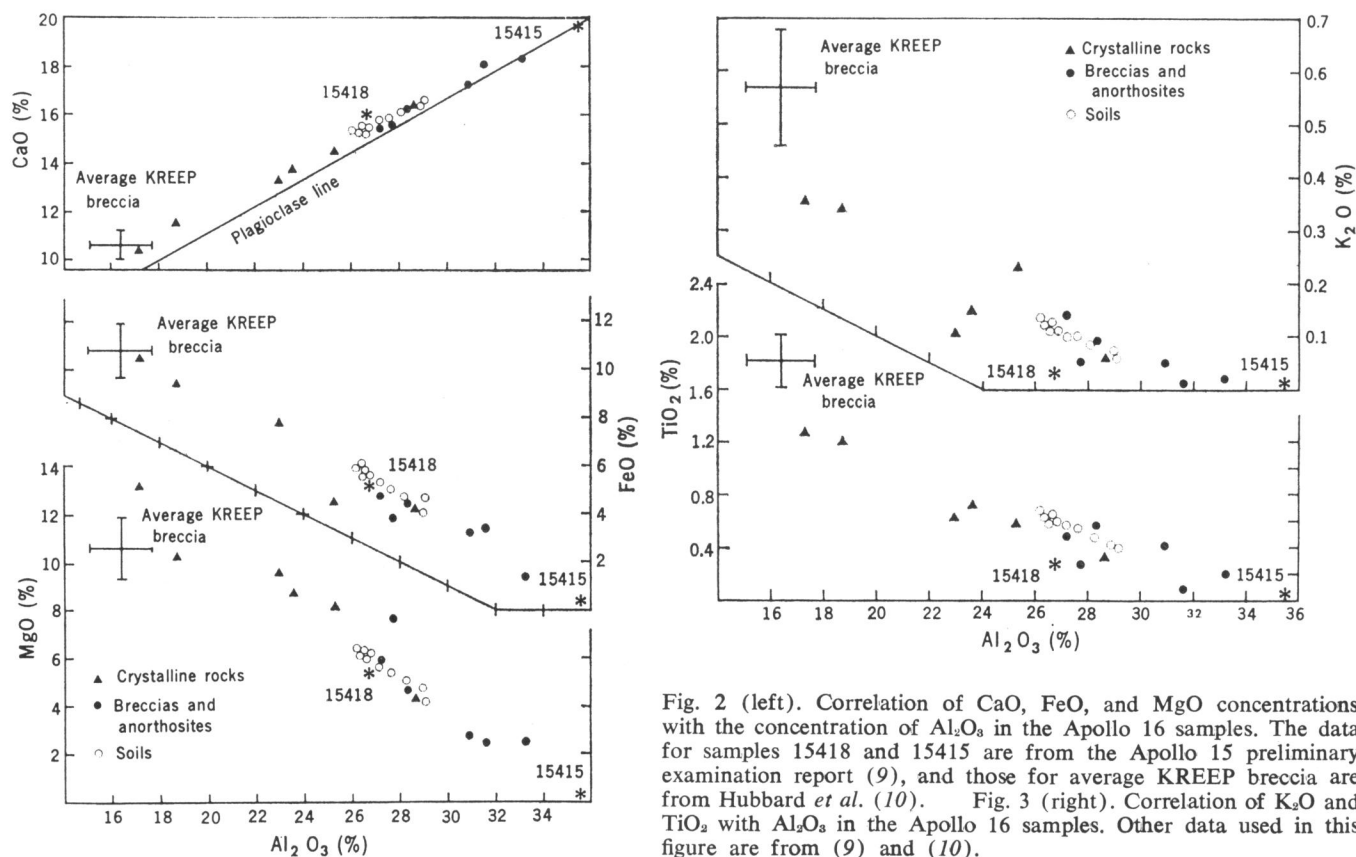
Fig. 2 (left). Correlation of CaO, FeO, and MgO concentrations with the concentration of Al_2O_3 in the Apollo 16 samples. The data for samples 15418 and 15415 are from the Apollo 15 preliminary examination report (9), and those for average KREEP breccia are from Hubbard et al. (10). Fig. 3 (right). Correlation of K_2O and TiO_2 with Al_2O_3 in the Apollo 16 samples. Other data used in this figure are from (9) and (10).

Fig. 4. Correlation of Nb, Yb, and Zr concentrations with the concentration of TiO_2 in the Apollo 16 samples. Note the nearly identical patterns of data points on these three graphs, indicating a marked correlation between Nb, Y, and Zr.

the high Y/Ti and Nb/Ti ratios suggest that the crystalline metaigneous component is relatively rare in the soil. The nickel content of the soils varies by more than a factor of 3. If the nickel abundance is an indicator of a meteoritic component and, thus, a measure of the maturity of the soil, the data suggest that some soils are probably associated with deep ejecta from young craters that have been less gardened than a typical soil from this region. The abundances of niobium, ytterbium, zirconium, and titanium are correlated with each other in both rock and soil samples, the correlation being particularly good within the soil samples. Data for these elements are illustrated in Fig. 4. The four complex breccia samples with Al_2O_3 contents similar to those of the soils have much more variable TiO_2, K_2O, Y, and Nb concentrations than the soils, indicating that they are derived from a more heterogeneous milieu.

Several additional generalizations and comparisons with other lunar materials may be inferred from the strontium, zirconium, ytterbium, nio-

bium, and thorium contents determined for the rocks from this site. Both mare and nonmare basaltic rocks are characterized by relatively high abundances of large quadrivalent and trivalent ions (such as thorium, the lanthanide elements, and zirconium) relative to divalent ions (such as europium and strontium). This characteristic is best illustrated by the commonly observed low abundance of europium relative to samarium and gadolinium. The inverse
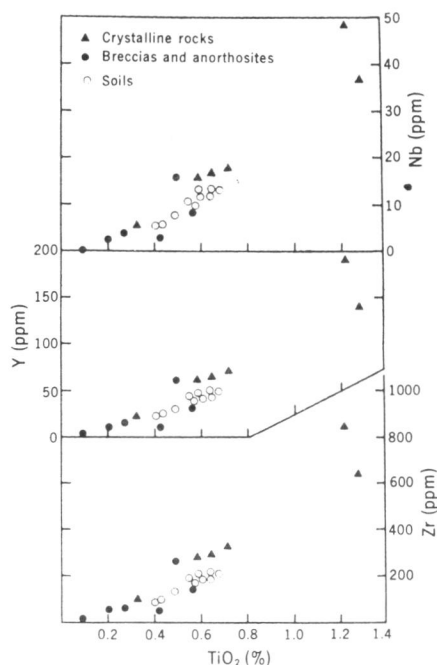
of this characteristic is observed in pure plagioclase and plagioclase-enriched materials returned from the lunar surface. The ubiquitous fractionation of these groups of elements on the lunar surface indicates that the separation of plagioclase from igneous liquids is common in igneous processes on the moon. The relatively high and relatively constant Sr content of most of the Apollo 16 samples, along with the highly variable and frequently low Zr, Y, Nb, and Th contents, suggests that these samples have been involved in processes where they have become enriched in plagioclase. The Y, Zr, Th, Nb, and Sr contents of samples 60315 and 62235 are distinctly different from those of all other samples and suggest that these rocks are depleted in divalent elements relative to trivalent and quadrivalent elements (that is, they are similar to other lunar basaltic rocks). Their relative abundances are, in fact, similar to those observed for KREEP basalts. The similarity of the trace element characteristics of these two rocks and those of primary magmas supports the conclusion that they represent a relatively undifferentiated magmatic rock. The concentrations of Y, Zr, Th, Nb, and Sr in samples 61156, 66095, and 60335 are intermediate between those found for rocks that are enriched in plagioclase, for example, sample 60016 and the "basaltic" rocks

Table 2. X-ray fluorescence analyses of Apollo 16 soils. Abbreviations used: Sta., station; %, percentage by weight; ppm, parts per million; N.D., not detected.

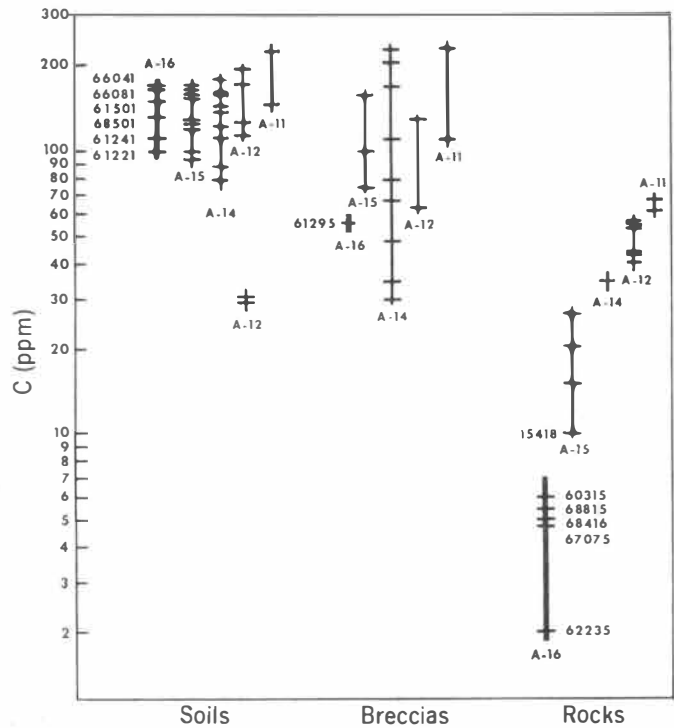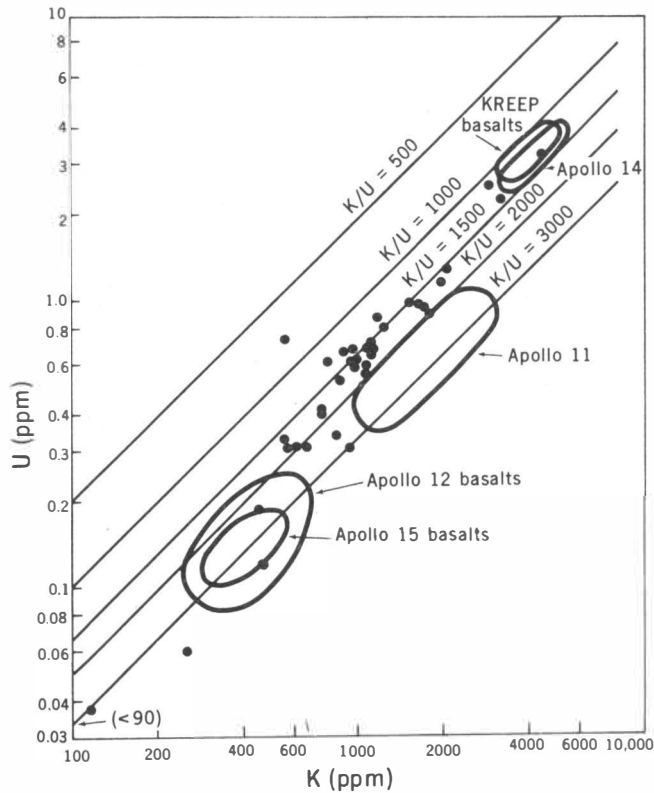| Component		LM rake soil 60600,2	Sta. 1 sub-surface white soil 61220,2	Sta. 1 upper gray soil 61241,2	Sta. 1 crater rim 61501,1	Sta. 4 trench bottom 64421,1	Sta. 5 rake soil 65701,2	Sta. 6 gray soil 66041,1	Sta. 6 white soil 66081,2	Sta. 11 fillet reference soil 67480,2	Sta. 11 crater rim rake soil 67600,1	Sta. 8 fillet reference soil 68841,2
SiO_2	(%)	45.35	45.35	45.32	44.66	44.88	45.03	45.07	45.38	44.95	45.28	45.08
TiO_2	(%)	0.60	0.49	0.57	0.56	0.55	0.64	0.64	0.67	0.41	0.42	0.59
Al_2O_3	(%)	26.75	28.25	27.15	26.50	27.60	26.47	26.39	26.22	29.01	28.93	26.49
FeO	(%)	5.49	4.55	5.33	5.31	5.03	5.87	6.08	5.85	4.66	4.09	5.65
MnO	(%)	0.07	0.06	0.07	0.07	0.06	0.08	0.08	0.08	0.06	0.06	0.07
MgO	(%)	6.27	5.02	5.75	6.08	5.35	6.02	6.14	6.39	4.20	4.75	6.27
CaO	(%)	15.46	16.21	15.69	15.33	15.81	15.29	15.29	15.28	16.54	16.40	15.30
Na_2O	(%)	0.38	0.42	0.55	0.41	0.39	0.41	0.38	0.39	0.42	0.44	0.41
K_2O	(%)	0.11	0.09	0.10	0.11	0.10	0.12	0.12	0.13	0.06	0.07	0.11
P_2O_5	(%)	0.13	0.10	0.13	0.11	0.13	0.13	0.15	0.13	0.13	0.06	0.12
S	(%)	0.07	0.06	0.07	0.08	0.07	0.09	0.09	0.09	0.09	0.03	0.04	0.08
Sum		100.68	100.60	100.73	99.22	99.97	100.15	100.43	100.61	100.47	100.54	100.17
Sr	(ppm)	173	182	175	167	172	173	167	170	188	194	169
Rb	(ppm)	2.9	2.4	2.7	3.0	2.9	2.9	3.0	3.1	1.4	1.3	3.1
Y	(ppm)	43	31	37	40	42	48	44	48	22	22	46
Th	(ppm)	1.9	2.6	1.2	2.2	2.8	1.9	2.6	3.2	N.D.	1.6	2.4
Zr	(ppm)	186	131	162	177	183	207	197	205	86	89	201
Nb	(ppm)	12	7.6	9.8	11	11	13	12	13	5.4	5.4	13
Ni	(ppm)	293	109	220	256	316	356	362	342	176	111	296
Cr	(ppm)	770	590	720	760	710	820	820	830	520	540	780

Fig. 5 (left). Uranium plotted against potassium concentration for the Apollo 16 samples, as compared to the general range of samples from previous missions. The data are from NASA Manned Spacecraft Center, Oak Ridge National Laboratory, and Battelle Laboratories.   Fig. 6 (right). Comparison of the total carbon abundances for the Apollo 16 sample types with those of samples from previous Apollo missions. The latter data are taken from the Apollo 12, Apollo 14, and Apollo 15 Preliminary Examination Team reports (9, 11) and Moore et al. (12).

60315 and 62235. Neither the trace element concentrations nor the major element compositions of these rocks excludes the possibility that they are derived from an undifferentiated, highly aluminous parent magma. This possibility is particularly interesting because it suggests that rocks representing the parent liquids for anorthosites may occur at this site. With the exception mentioned above, the chemistry of the Apollo 16 rocks can be accounted for by a rather simple geologic model consisting of a large, igneous complex that is variably enriched in plagioclase and intruded by a liquid rich in trace elements after its formation.

The abundances of potassium, uranium, thorium, and short-lived radioactive elements have been determined for 43 rock and soil samples. These data show that the Th/U ratio of highland materials, like that of most mare samples, is similar to that of chondrites. The K/U ratios of all but two samples from this site fall within the range 1000 to 2000. These data are compared with the potassium and uranium contents of rocks from previous landing sites in Fig. 5. Even though the rocks and soils from the Apollo 16 highland site are relatively low in

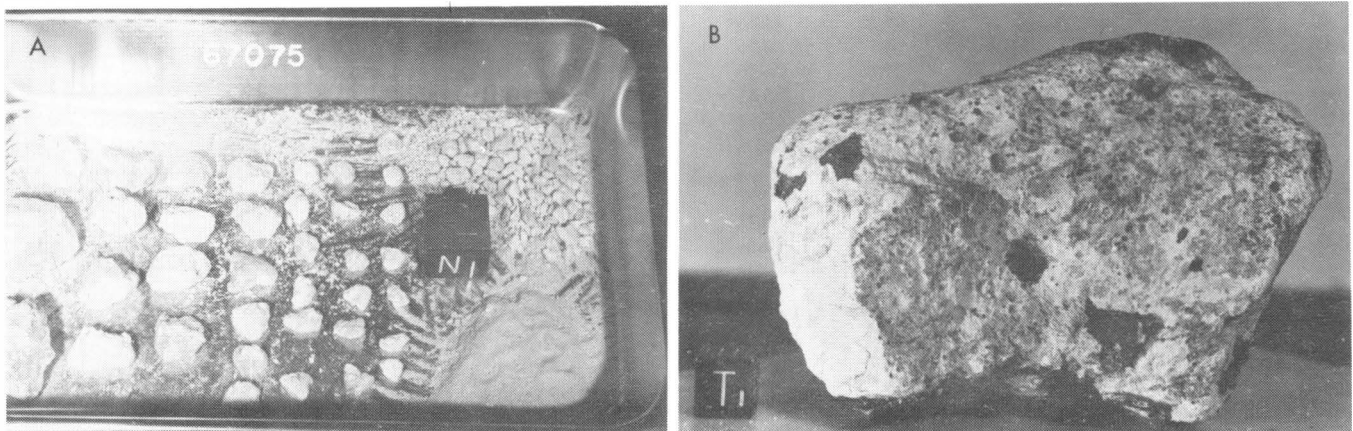Fig. 7. Typical examples of type II rocks. (A) Sample 67075 shows the extremely friable nature of this material, which was collected as a single rock on the lunar surface. The cube shown is 1 cm on an edge. (B) Sample 65315 is a more coherent but still friable rock of crushed plagioclase. Note the preserved glass-lined impact pits on the "weathered" surface. A few remnants of a black glass coating remain.
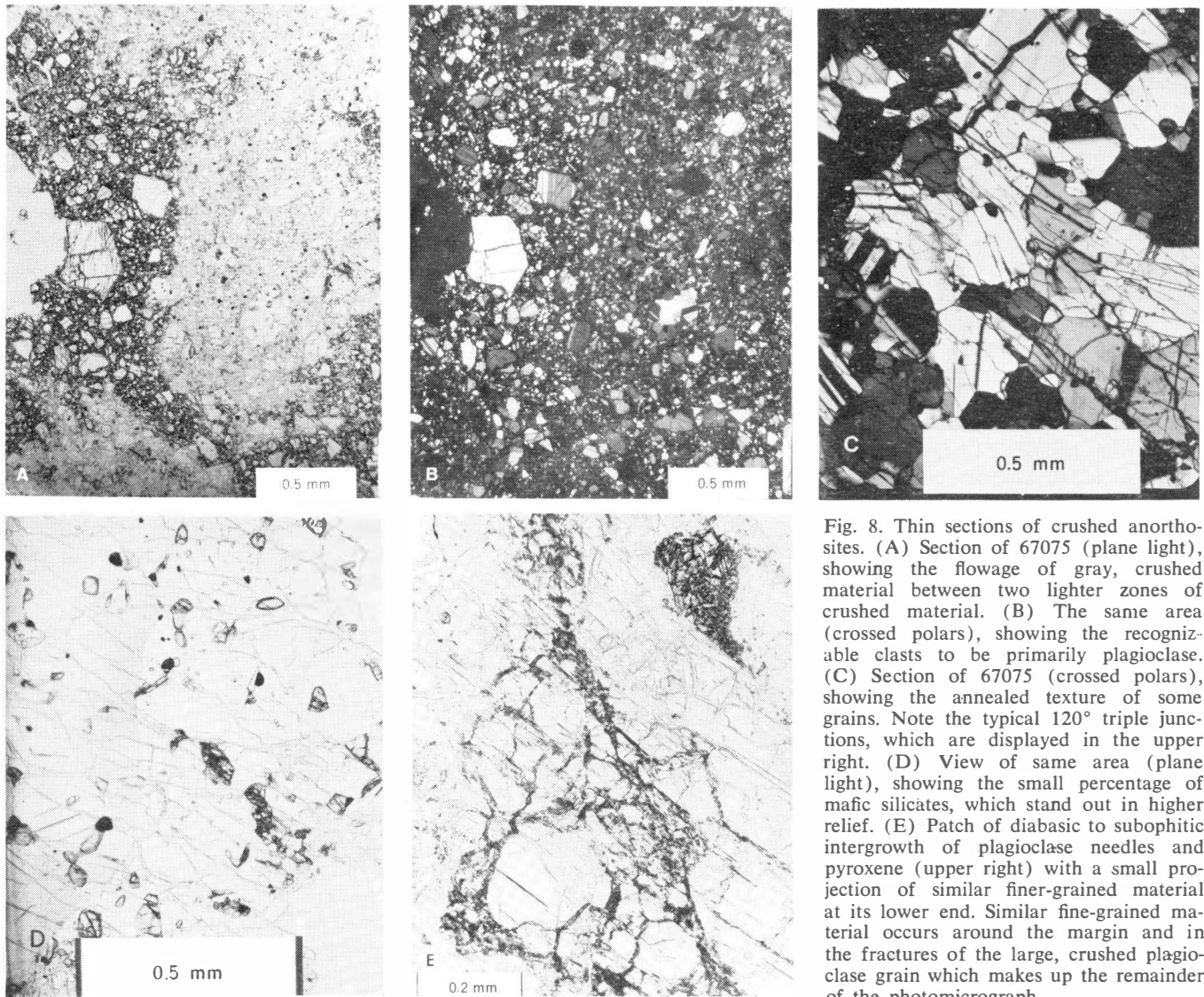
Fig. 8. Thin sections of crushed anorthosites. (A) Section of 67075 (plane light), showing the flowage of gray, crushed material between two lighter zones of crushed material. (B) The same area (crossed polars), showing the recognizable clasts to be primarily plagioclase. (C) Section of 67075 (crossed polars), showing the annealed texture of some grains. Note the typical 120° triple junctions, which are displayed in the upper right. (D) View of same area (plane light), showing the small percentage of mafic silicates, which stand out in higher relief. (E) Patch of diabasic to subophitic intergrowth of plagioclase needles and pyroxene (upper right) with a small projection of similar finer-grained material at its lower end. Similar fine-grained material occurs around the margin and in the fractures of the large, crushed plagioclase grain which makes up the remainder of the photomicrograph.

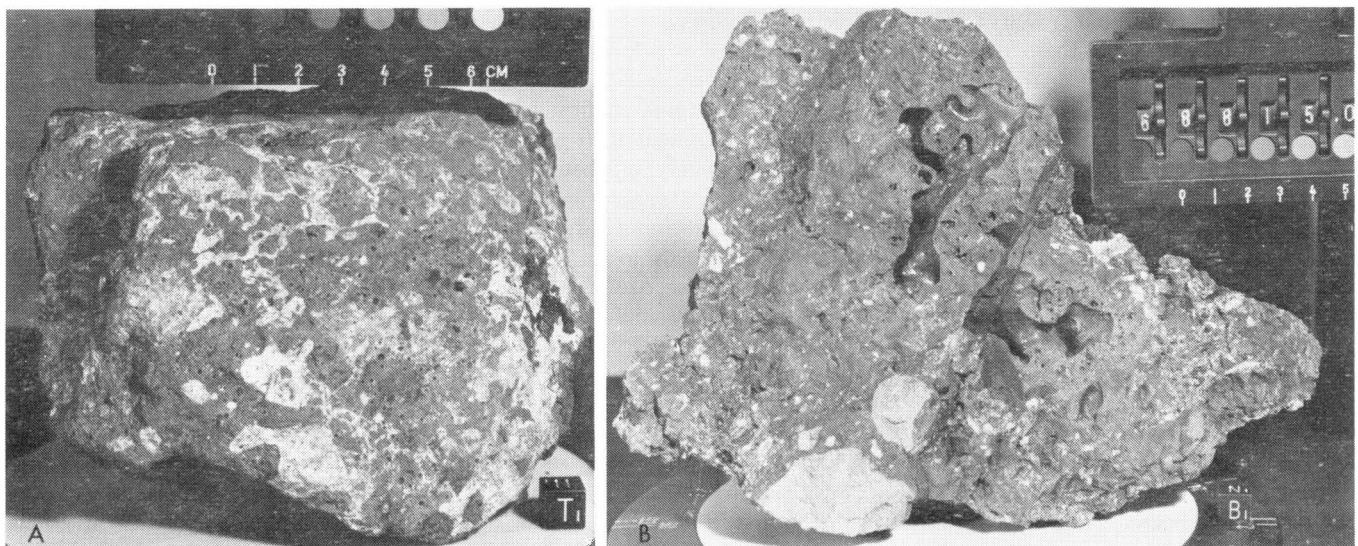Fig. 9. Complex gray and white breccias. (A) Rock 61015 shows the complex arrangements in which some areas show white clasts in a gray matrix, but others have gray clasts in a white matrix. (B) Rock 68815 shows the predominantly gray version of this rock type. Note the striking tubular vesicles, which indicate the once fluid nature of this rock. Smaller vesicles are concentrated along margins of tubes.

potassium, they have similar K/U ratios to the KREEP basalts and distinctly lower K/U ratios than most mare basalts. These data are in accord with the suggestion that the older and shallower parts of the moon have lower K/U ratios than the deeper interior, which presumably produced the mare basalts.

The carbon contents of 12 soil and rock samples are given in Fig. 6, along with data from previous sites. The soil samples from the Apollo 16 regolith have carbon contents similar to those of most lunar soils. In contrast, the rock samples have carbon contents no more than one-half those of most mare basalts. This difference may be due to (i) a very low carbon content of highland, crustal materials, or (ii) extensive degassing of all samples during their formation. The latter explanation is quite unlikely for the cataclastic anorthosites, which show only minimal evidence of thermal metamorphism. We conclude therefore, that many of the highland rocks are derived from a source rock with a distinctly lower carbon content than most mare basalts. These additional data on the carbon regime of the lunar surface further support the hypothesis that the bulk of the carbon found on the lunar surface originates from the solar wind.

Petrographic Characteristics

Both visual and microscopic examinations show that the coherent rocks from the Apollo 16 site are highly variable in character and complex in origin. Most have macroscopic and microscopic textures that result from two or more events in their history. Cataclastic, highly crushed rocks are common, in addition to complex intergrowths of shock-produced glass, devitrified glass, and preexisting clasts. Other rocks seem to be the product of simple thermal recrystallization, with textures resembling those near large, igneous intrusions. None of the rocks have the hallmarks of lavas or hypabyssal rocks that were so evident in the Apollo 11, Apollo 12, and Apollo 15 mare basalts. To date, petrographic studies of Apollo 16 rocks have uncovered only two or possibly three specimens that can be unambiguously categorized as holocrystalline, igneous rocks. The scarcity of such rocks at this site is well illustrated by the astronauts' descriptions while they were

on the surface. Astronaut Duke commented while driving to station 1 during the first extravehicular activity, "I haven't seen any [rock] that I'm convinced is not a breccia."

In the preliminary examination all the rock samples, including several hundred fragments collected with a raking tool, were cleaned to remove dust coatings from their surfaces. The surfaces were then examined visually and with a low-power binocular microscope. In addition, petrographic thin sections of 35 specimens were studied by conventional petrographic methods. Four rather broadly defined rock types can be identified from this examination:

1) Cataclastic anorthosites (type II) (7).

2) Partially molten breccias (type IV).

3) Igneous and high-grade metamorphic rocks (type III).

4) Polymict breccias (type I).

Cataclastic Anorthosites (Type II)

This type consists of white, generally friable, highly brecciated, anorthositic rocks. Degrees of coherence in this group vary; some samples, during transit and handling, have broken into many fragments (Fig. 6A), while others have remained as single fragments (Fig. 7B). Examined under the binocular microscope, these rocks appear to consist of 70 percent (or more) plagioclase in the form of clear, gray, or white grains (generally all three types occur in each specimen), and a few light yellow to honey brown to light green minerals. Most of the rocks have partial to nearly complete dark gray, vesicular, glass coatings, much of which has been lost through micrometeorite erosion. Observations of thin sections confirm a very high plagioclase content with pyroxene and olivine in highly crushed or annealed textures that suggest cataclastic deformation of anorthositic fragments. A question that needs to be answered for this category is: Are all of these rocks cataclastically deformed fragments, or are some detrital in origin? Differing degrees of coherence and relations of different types of plagioclase grains may be associated with differing degrees of shock and may be geographically distributed in a meaningful way. Our first impression is that the most friable and least coherent white rocks were collected at the rim of North Ray crater.

The extremely crushed nature of the plagioclase in thin section is illustrated in Fig. 8, A and B. In Fig. 8A, it appears that the crushed material of the darker area was behaving as a fluid and was squeezed between the two lighter areas. The somewhat annealed nature of the crushed plagioclase is seen in Fig. 8C, where some of the grains meet at triple junctions. The small percentage of mafic silicates is shown in Fig. 8D. Indications of partial melting are present in this rock type. Small patches with diabasic to subophitic textures occur interstitially to some plagioclase grains. Small veinlets of finer grain size occur sporadically as offshoots from these patches. Similar veins often occur along parts of the margins of plagioclase grains, or as veins in them (Fig. 8E). Apparently, the white, clear, and gray areas seen under the binocular microscope represent partly crushed plagioclase, diaplectic glass, and partially melted zones, respectively. Some specimens of this type of rock contain a somewhat higher percentage of mafic silicates, but are still in the range of anorthositic rocks (more than 70 percent plagioclase). For example, samples 67955, 64435, and 60025 have at least 10 percent olivine as subhedral grains, both as small inclusions in plagioclase and as larger grains in pyroxene, which is interstitial to plagioclase. These rocks are highly crushed, but thin sections display a few areas in which the original texture is preserved. They were probably troctolitic anorthosites.

Some special problems are posed by these cataclastic rocks. There is evidence that they retain relicts of a much coarser-grained fabric. The relicts suggest that, although the grains are intensely crushed, the rocks were not necessarily highly stirred and may retain discernible preshock textures. The relicts are generally most evident in plagioclase, but they can also be seen in mafic minerals. For instance, in sample 60025 the orthopyroxene is generally much coarser than olivine and of a size comparable to the largest plagioclase relicts. The olivine grains can be arranged in a series in which progressive polygonalization and rotation of small blocks is seen. The series suggests that the original average grain size of olivine was at least as large as the largest mildly polygonalized grains and was probably comparable to that of orthopyroxene. Such grain sizes and shapes are a clue to the preshock nature

of the rocks, which may be parts of the original lunar crust.

In 67955, a clearly discernible relict cumulus texture is evident in the form of extensive orthopyroxene oikocrysts, which enclose ovoid olivine and plagioclase. Early ovoidal olivine, without an orthopyroxene mantle, is enclosed in plagioclase. The whole specimen (as judged from a view of the thin section under low magnification) appears to have a lamination which may be relict layering; like the relicts of coarse-grained texture, this indicates that this rock and probably others were not necessarily highly stirred when they were shocked.

Partially Molten Breccias (Type IV)

This type consists of a rather complex series of breccias containing white and gray material. In some cases it appears that the white material is matrix that contains gray clasts, while in other cases it appears that the gray material is matrix that contains white clasts. In many instances, these two cases occur in the same rock (Fig. 9A). The proportions of white and gray material vary considerably from one specimen to another. For example, samples 68815 and 60017 consist primarily of the dark material, but show a few small spots of white (Fig. 9B).

These two rocks also contain long, worm-like, tubular vesicles. In 68815 there is a higher proportion of white material, which occurs for the most part as distinct clasts in the dark matrix, but other portions of this same rock have larger white areas in which a few gray fragments occur. A frothy, vesiculated zone also occurs on one side of this rock.

The dark material is aphanitic and, under the binocular microscope, is suggestive of devitrified glass. Thin sections confirm this but also show varying amounts of mineral debris as well as small, fine-grained, gray clasts included in the flow-banded devitrified glass. In some areas, the gray material consists of many rounded to angular fragments of plagioclase in a finer-grained matrix containing many needles of plagioclase randomly arranged as though crystallized from a melt (Fig. 10A). The rather ragged edge of the large white plagioclase area in contact with the small needle-bearing matrix, the small islands of plagioclase that seem to have been wedged off the lower edge of the plagioclase arm (Fig. 10A, upper left), and the small dike-like embayment on the upper edge of the arm all lead to the conclusion that the gray material was, at one time, in large part melted. It is similar in composition to anorthositic rocks (Table 1). The white material, anorthositic in composition, is in various stages of brecciation or recrystallization.

It seems clear that there is a heterogeneous set of gray and white, partially melted rocks that are found throughout the landing site. Perhaps these rocks are part of a series in which varying degrees of melting and assimilation of clasts and fine debris have occurred. The white clasts may have been granulated to the point where they behaved mechanically as a fluid and were squeezed into the partially melted matrix as veins and blebs, which may, in turn, have picked up a few fragments of the dark material (Fig. 10B). Some of the white clasts have not been significantly deformed and contain textures that probably reflect a previous environment. One of these in rock 67434 contains subhedral olivine and pink spinel in a poikilitic plagioclase matrix (Fig. 10, C and D). It should be noted that many of the olivines in the Apollo 16 rocks have unusually low interference colors and are difficult to distinguish from orthopyroxene.
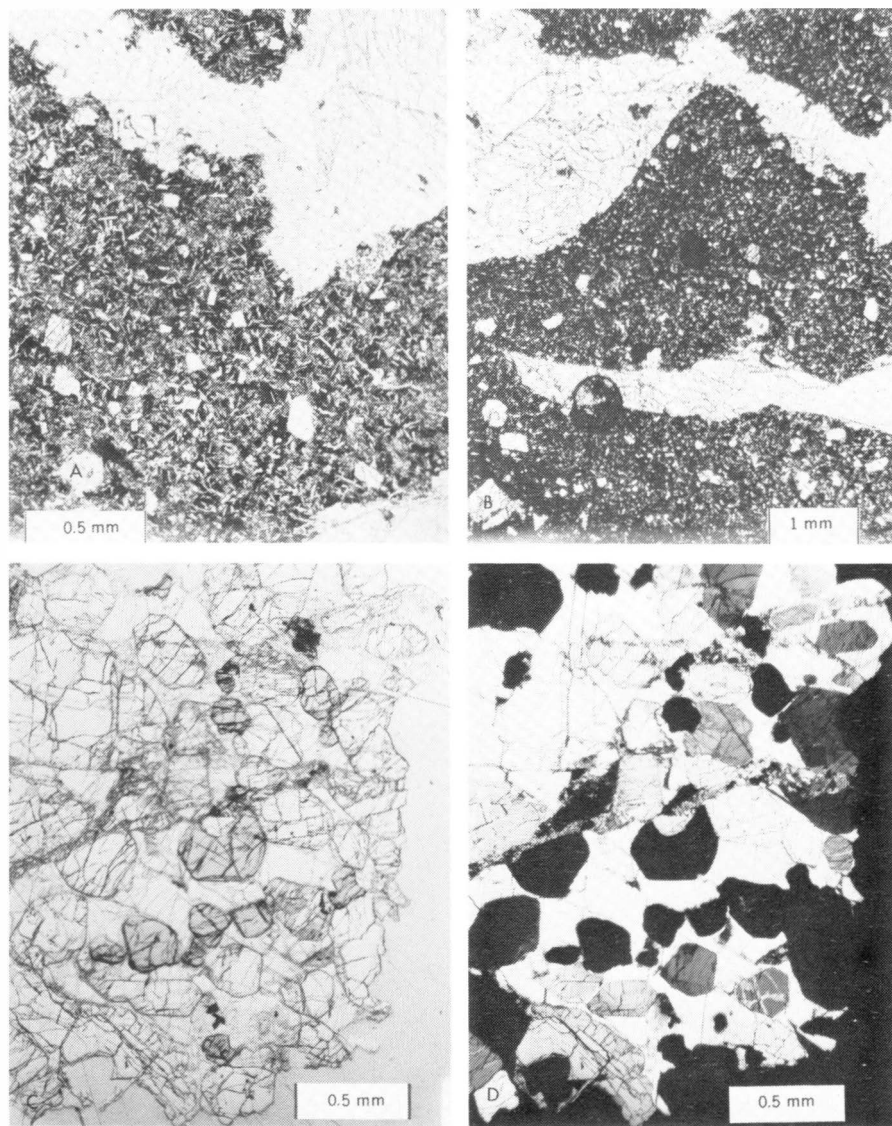
Fig. 10. Complex gray and white breccia. (A) Sample 61015 (plane light), view of a white vein through a gray area. Plagioclase occurs in the gray material as both small needles and larger, rounded to angular fragments (see text). (B) View of a larger area of the same section showing the vein-like nature of the white crushed plagioclase. (C) Clast from 67435 (plane light), view of plagioclase (very light gray), subhedral olivine (light gray), and spinel (gray). (D) View (crossed polars) to illustrate the isotropic nature of the spinel and the poikilitic nature of the plagioclase.

Igneous and High-Grade Metamorphic Rocks (Type III)

This type includes a variety of homogeneous, coherent, crystalline rocks. The greatest variation in chemical composition of the Apollo 16 rocks occurs in this group. Again, there is a general predominance of plagioclase, which seems to be present in quantities that normally range upward from about 70 percent, although in some instances the percentage of mafic minerals is significantly greater and in two of the rake samples (67667 and 64815) approaches that of an ultramafic rock. The grain size is generally of the order of a millimeter or less. In some rocks (such as 68415, 68416, and 65015) the plagioclase is euhedral, while in others (such as 61156 and 65095) it is anhedral. Light green or yellow to honey brown mafic materials are seen in most of this group under the binocular microscope. Examinations of thin sections of this type indicate that there are two major subgroups. One subgroup contains euhedral plagioclase laths of various sizes plus pyroxenes and perhaps olivine in a texture indicative of crystallization from a melt. The plagioclase occurs both as well-developed laths in a diabasic texture complete with large phenocrysts (Fig. 11A) and as skeletal crystals that formed during rapid cooling from a melt from which plagioclase, olivine (orthopyroxene?), and spinel (Fig. 11B) crystallize. The other subgroup has large poikilitic pyroxene grains, which include plagioclase and other mafic minerals (Fig. 12, A and B). The poikilitic grains are made up of numerous individual, irregularly shaped areas of pyroxene. The texture is indicative of recrystallization, as in a metamorphic hornfels.

An interesting observation on rock 66095 of the second subgroup is the alteration of numerous areas where the original phases have taken on a rusty appearance. In many instances, the rust penetrates as a stain into the zone around these phases. The rust-like material also forms a very thin crust along some fracture surfaces. Its optical properties in polished thin sections are those of goethite. Although it appears that some of this alteration must have occurred on the lunar surface, it remains to be determined how much of it might result from exposure to the atmospheres of the spacecraft and earth during the return trip.

Polymict Breccias (Type I)

This type consists of polymict breccias with a white to very light gray, moderately friable, clastic matrix, in which material with a grain size of less than a few tenths of a millimeter predominates (Fig. 13). The matrix appears to be a more crushed equivalent of the clast materials and is essentially free of glass. Clasts in these breccias are generally of the order of a few millimeters in size, although rarely there may be clasts a few centimeters across. The clasts range from very white and plagioclase-rich, through various shades of gray, to medium dark gray and aphanitic. The lighter clasts may contain up to 20 or 30 percent mafic minerals, and they range from
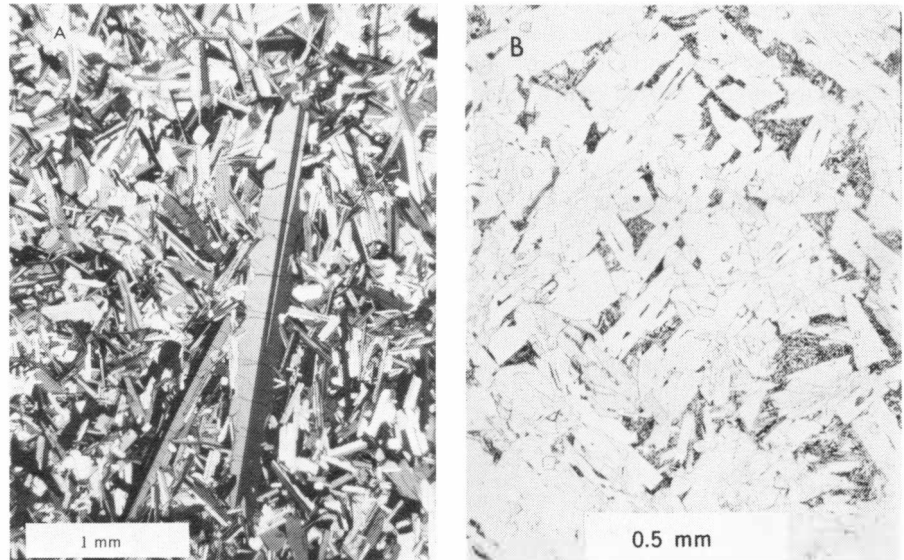

Fig. 11. Igneous crystalline rocks. (A) Sample 68416 (crossed polars), view showing euhedral plagioclase laths both as phenocrysts and in a diabasic matrix, which also contains about 20 percent pyroxene as smaller, irregularly shaped grains between the laths. (B) Sample 62295 (plane light), view showing skeletal plagioclase laths, with interstitial plagioclase and olivine (orthopyroxene?) that formed from a trapped interstitial melt. The mineral seen in higher relief as small, euhedral, inclusions in the large plagioclase grains is spinel.
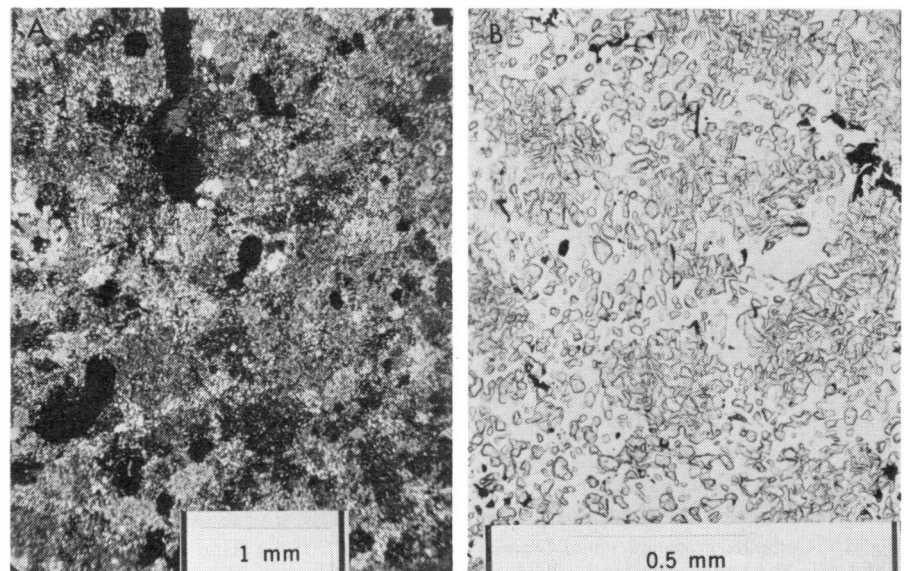

Fig. 12. Poikilitic crystalline rocks. (A) Sample 61156 (crossed polars), view showing irregularly shaped poikilitic patches of pyroxene accented by the different shades of gray. Each of the patches contains numerous individual grains, as shown in the higher magnification in (B), a plane light view of a highly magnified area of one poikilitic crystal.
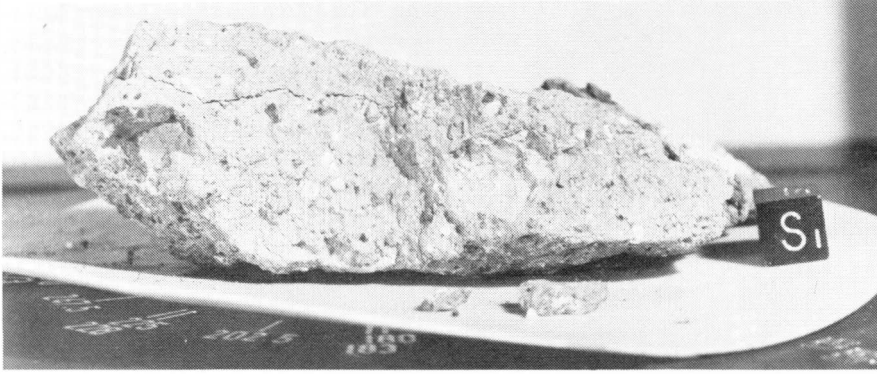
anorthositic to gabbroic, noritic, or troctolitic in composition. The darker clasts may be devitrified glass and rarely contain small white spots. The distribution of various clast types appears to vary from sample to sample.

This category is typified by samples 60016, 60019, 61135, 61175, 61295, 66035, and 66075. Other specimens that are similar include 63355, 67015, 67016, and 67115, which are lighter in color, more coherent, and contain predominantly aphanitic dark gray clasts of a larger size. Still other specimens, such as 65786, 65925, and 61525, display a slightly darker color and are somewhat more coherent than the typical type. However, the matrix and variety of small clasts appear to be similar in all subgroups. It may be significant that the lighter-colored subgroup occurs in the northern part of the landing site at stations 11 and 13, while the more typical examples occur farther south.

Thin sections of this type show the matrix to consist entirely of crushed mineral fragments with essentially no glass, even down to a very fine scale. Although there is a variety of clast types, the predominant one is plagioclase, as one would predict from the chemical analysis of sample 61295 (Table 1). The plagioclase clasts exist as large, ragged, single crystals, annealed aggregates, finely crushed material, and some maskelynite (Fig. 14). The various gray, aphanitic clasts seen under the binocular microscope apparently consist of finely crushed plagioclase aggregates or devitrified glass. Finally, there are a few clasts containing poikilitic pyroxene and some consisting of glass.

The clast population of these rocks is, at the present level of examination, similar to those of the other rock types found at this site. Except for the near absence of glass, the characteristics of

these rocks, including the moderately high carbon content of one analyzed example of this type, suggest that they are indurated equivalents of local regolith. The variability of the TiO_2 and K contents, in contrast to the smooth trends exhibited by the present surface soils (Fig. 3), suggests that these rocks are derived from a more heterogeneous source than the present regolith.

Glass and Opaque Minerals

In addition to the four rock types listed above, there are several forms of glass; these include two glass spheres, 60095 and 65016, the latter being hollow. Other predominantly glass samples are generally vesicular agglutinates. In addition, we note that both type IV and type II are commonly coated with a dark gray glass. Types I and III do not show such coatings. A thin section of this glass shows a high degree of devitrification, much of which appears to be plagioclase, but the fine-grained nature of the crystals makes their identification difficult.

The opaque mineral content of most rocks of types II and IV is generally low compared to that of rocks from other landing sites, ranging from less than 1 percent to less than 0.01 percent. The cataclastic anorthosites contain the lowest opaque mineral content of the four rock types; sample 65315 contains no more than about 0.001 percent opaque minerals. The poikilitic rocks of type III contain the highest contents of ilmenite; it is consistently present in amounts greater than about 2 percent. Rock 63335 contains even greater amounts. The high ilmenite content is a reflection of the relatively high titanium content of this group.

In the Apollo 16 rocks, unlike most rocks from previous missions, metal

and troilite commonly predominate over opaque oxide minerals; but generally the metal and troilite contents do not appear to be exceptionally high for lunar breccias. In no rock examined was the metallic iron content greater than about 1 percent. Ilmenite is commonly the dominant oxide mineral. The shapes and sizes of the ilmenite grains provide a useful index for determining the degree of crystallinity of the breccias.

Discussion of Petrography

The textural characteristics suggest that types II and IV may not be clearly distinguishable. They may form a continuous series ranging from crushed anorthositic rocks with little or no partial melting to those with a high degree of melting and crushing. The similarities in mineralogy, clast types, chemical composition, and textural gradations all argue for such a continuous series. Some rocks are nearly all white, crushed anorthosite, and others are nearly all gray, partially melted anorthosite; the entire range of white and gray mixtures between these extremes can be observed. Many of these rocks seem to be cataclastically crushed, preserving relict textures of the original rocks; but others seem to be more highly brecciated and melted, leaving only a few clasts with a clue to the texture of the original rocks. Nevertheless, the clasts are similar to the relict cataclastic textures in their anorthositic affinities, both mineralogically and texturally. Moreover, the textures of the rocks of types II and IV suggest that these rocks are distinct from all other lunar breccias. They contain no evidence that they are mechanically produced mixtures of pre-existing rocks. They are monomict rather than polymict breccias in the sense that these terms were used by Wahl (8) to describe meteorites. They exhibit peculiar melting textures, perhaps related to macroscopic or submacroscopic heterogeneities. The molten parts, whether they are the major portions of the type IV rocks or small molten portions within the type II

rocks, are generally richer in iron and magnesium than the surrounding or enclosed material. We suggest that the heterogeneous occurrence of mixtures with lower melting temperatures determined whether or not particular parts of a rock underwent melting. Thus, the early melting patches in some rocks may, in fact, represent late crystallizing interstitial liquids in a coarse-grained anorthositic cumulate. No chemical analysis was made of the glass coating on types II and IV, but it may well be similar to the anorthositic rocks of groups II and IV and represent the nearly totally melted equivalent of the gray areas in these rocks.

These descriptions of the rocks indicate that rock types II and IV originated from a relatively coarse-grained, igneous complex consisting predominantly of anorthosite, which was directly transformed to the observed rocks by impact or cataclysmic metamorphism. Some of the anorthosite was troctolitic, as indicated by the early euhedral crystallization of olivine in some rocks and clasts. The rare ultramafic rocks among the rake samples may be related to this complex either as small layers or as sparse fragments from a greater depth. Although the original source area for these particular rocks is uncertain, it does not appear to be in the upper few tens of meters beneath the landing site. This conclusion is based on the photographs of North Ray crater, which contains boulders of breccia; the ejecta from North Ray and South Ray craters; and the interpretation of the active seismic experiment data. Nevertheless, the widespread distribution of
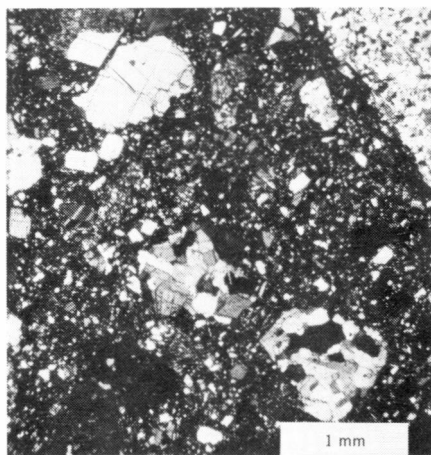

Fig. 14. Thin section of rock 61295 (crossed polars). The clasts show the variety of plagioclase assemblages: finely crushed (upper right); annealed (lower center); large, ragged single crystal (upper left).

the series of rock types II and IV over both mountains and plains areas and the similar widespread conformity of the soil composition, which ranges from anorthositic gabbro through gabbroic anorthosite and represents the homogenizing and reworking of many layers of material in the upper few hundred meters of the entire area, suggest that the area is underlain at some depth by an anorthositic complex.

The origin of at least some of the type III rocks—in particular, those with KREEP basalt chemistry—may be unrelated to the anorthosites. The igneous rocks 68416 and 68415 are two chips (separated by 20 to 30 cm) from a large boulder. Even though these specimens are from a single rock, they are appreciably different in grain

size. The parent rock may represent a portion of a pool of impact molten material rather than an unshocked part of the underlying anorthosite. In this case the two chips are genetically the extreme end members of the type II-IV series.

Reviewing the classification of the Apollo 16 rock specimens in terms of their petrogenesis, we find three major types:

1) A series of cataclastically and cataclysmically modified anorthositic rocks, probably derived from an anorthositic complex which contained from 70 to 90 percent plagioclase.

2) Igneous rocks, at least some of which underwent thermal metamorphism.

3) Polymict breccias that are mechanical mixtures of the preexisting rock types.

None of the returned samples are in accord with the preflight hypotheses concerning the origin of the landform units in this region. The rocks that apparently underlie the regolith of the plains region are in no sense volcanic. No evidence for lava flows or pyroclastic rocks was observed. The only possible rocks that could correspond to the Descartes volcanic unit presumed to underlie the hilly region to the north and southeast of the landing site are the high-alumina, igneous rocks (such as 66095 and 61156) or the KREEP basalts, which have metamorphic textures. The absence of sharp compositional gradients over the surface argues against the latter possibility. The more detailed study of soils and rake samples from stations 5 and 6 should clarify this conjecture.

Table 3. Comparison of the fractions in the size range 62.5 to 125 μm. Values are given as percentages by weight.

Component	Sample number and number of grains								
	61220 (100)	64421 (100)	66041 (105)	66081 (174)	68820 (100)	68841 (100)	69940 (100)	67480 (100)	67600 (100)
Agglutinates	8	54	39	53.4	52	80	64	24	20
Colorless glass fragments	23	3	3.8	9.8	2	2	4		3
Colorless glass droplets	2	1		1.7	1				2
Brown glass fragments				2.9		2	6	3	1
Brown glass droplets		1		1.7	Trace			1	Trace
Orthopyroxene				2.9	2		1	4	
Clinopyroxene	8	1	2.8			3	1	5	3
Plagioclase	35	15	16.1	9.2	15	7	7	22	22
Metamorphosed breccia	12	17	21.9	7.5	21	6	7	15	21
Vitric breccia	10	7	15.2	9.8	1	Trace	7	24	22
Anorthositic					6		2	1	5
Basalt	1	1		0.6		Trace	1		1
Olivine	1								
Ilmenite			0.9						
Potassium feldspar (?)				0.6					

Soil Characteristics

The fractions of 32 soil samples in the size range greater than 1 mm were examined surficially. For nine of these soil samples thin sections of the fraction smaller than 1 mm were further investigated. The fragments observed in these studies can be grouped into (i) glass-coated particles (agglutinates), (ii) mineral or lithic fragments that largely correspond to the rock types mentioned above, and (iii) a variety of vitric fragments. The lithic fragments include the breccias described above and the cataclastic anorthosites. Discrete mineral fragments of plagioclase, clinopyroxene, orthopyroxene, and olivine are relatively common. Trace quantities of pink spinel and potassium feldspar were also found. The prevailing glass type is colorless with a relatively high refractive index. Brown or colored glasses are much rarer at this site than they were at other Apollo landing sites.

The relative abundances of glassy and crystalline fragments are given for nine soil samples in Table 3. The abundance of glass varies rather markedly.

The median grain size of most soil samples ranges from 76 to 112 micrometers. However, the two samples from North Ray crater (67480 and 67600) and one whitish soil from station 1 (61220) are much coarser; their median grain size ranges from 250 to 300 μm.

It is noteworthy that the three coarser soils all have relatively low abundances of agglutinates as well as relatively low nickel contents. The concurrence of these three parameters suggests that these soils have been subject to gardening for a much shorter time than the typical soil. The occurrence of an immature soil (61220) in the bottom of the trench at station 1 suggests that remnants of relatively young rays from North Ray crater may be overlain by mature soils ejected from small, shallow craters. If this interpretation of the North Ray soils is accepted, they are clearly distinguishable from soil interpreted as South Ray ejecta which contains dark brown to black, vesicular glass droplets and dark gray breccias.

The core samples collected during the mission are summarized by Hörz et al. (5). Of particular note are the three sets of cores taken within 100 m of each other in the area of the LM and the Apollo lunar surface experiments package (ALSEP). The x-radiographs of the cores indicate that some correlations are possible between them, which will enable us to make the most detailed reconstruction of the lunar soil strata to date. The nature of the Descartes material may be classified by the core at station 4. Because of the ubiquitous covering of South Ray ejecta on Stone Mountain, the sampling of Descartes material on the surface is difficult. The x-radiographs of the station 4 material indicate a distinct change in grain size, abundance of rock fragments, and rock types at a depth of about 51 cm. It is possible that the underlying 20 cm of soil may contain evidence of any differences in chemical or mineralogical components in the Descartes material.

Summary

The preliminary characterization of the rocks and soils returned from the Apollo 16 site has substantiated the inference that the lunar terra are commonly underlain by plagioclase-rich or anorthositic rocks. No evidence has been found for volcanic rocks underlying the regolith in the Apollo 16 region. In their place, we have found anorthositic rocks that are thoroughly modified by crushing and partial melting. The textural and chemical variations in these rocks provide some evidence for the existence of anorthositic complexes that have differentiated on a scale of tens to hundreds of meters.

The occurrence of deep-seated or plutonic rocks in place of volcanic or pyroclastic materials at this site suggests that the inference from physiographic evidence that the latter materials are widespread in terra regions may be incorrect.

Several additional, more specific conclusions derived from this preliminary examination are:

1) The combination of data from the Descartes region with data from the orbital x-ray fluorescence experiment indicates that some backside, highland regions are underlain by materials that consist of more than 80 percent plagioclase.

2) The soil or upper regolith between North Ray and South Ray has not been completely homogenized since the time of formation of these craters.

3) The chemistry of the soil indicates that rocks rich in potassium, uranium, and thorium, similar to those that prevail at the Fra Mauro site, are relatively abundant (10 to 20 percent) in the Descartes region.

4) The K/U ratio of the lunar crust is similar to that of the KREEP basalts.

5) The carbon content of the premare lunar crust is even lower than that of the mare volcanic rocks.

References and Notes

1. D. A. Papanastassiou and G. J. Wasserburg, *Earth Planet. Sci. Lett.* **11**, 37 (1971); G. Turner, *ibid.*, p. 169; G. J. Wasserburg and D. A. Papanastassiou, *ibid.* **13**, 97 (1971); V. R. Murthy, N. M. Evenson, B. Jahn, M. R. Coscio, Jr., *Science* **175**, 419 (1972).
2. W. K. Hartman, *Icarus* **13**, 299 (1970).
3. N. J. Trask and J. F. McCauley, *Earth Planet. Sci. Lett.* **14**, 201 (1972).
4. C. A. Hodges, *Miscellaneous Geological Investigations Map I-748* (U.S. Geological Survey, Washington, D.C., 1972); D. E. Wilhelms and J. F. McCauley, *Miscellaneous Geological Investigations Map I-703* (U.S. Geological Survey, Washington, D.C., 1971).
5. F. Hörz, W. D. Carrier, J. W. Young, C. M. Duke, J. S. Nagle, R. Fryxell, in preparation.
6. C. Meyer, Jr., R. Brett, N. J. Hubbard, D. A. Morrison, D. S. McKay, F. K. Aitken, H. Takeda, E. Schonfeld, *Geochim. Cosmochim. Acta* **1** (Suppl. 2), 393 (1971); C. Meyer, Jr., Contribution 88, Lunar Science Institute (1972), p. 542.
7. Arabic numerals represent the order of presentation in this paper. Roman numerals were developed during the preliminary examination and have been retained because they appear in several documents circulated to principal investigators by the lunar sample curator.
8. W. Wahl, *Geochim. Cosmochim. Acta* **2**, 91 (1952).
9. Apollo 15 Preliminary Examination Team, *Science* **175**, 363 (1972).
10. N. J. Hubbard, J. M. Rhodes, P. W. Gast, B. M. Bansal, H. Wiesmann, S. E. Church, in preparation.
11. Lunar Sample Preliminary Examination Team, *Science* **167**, 1325 (1970); Lunar Sample Preliminary Team, *ibid.* **173**, 681 (1971).
12. C. B. Moore, E. K. Gibson, J. W. Larimer, C. F. Lewis, W. Nichiporuk, *Geochim. Cosmochim. Acta* **2** (Suppl. 1), 1375 (1970).

Spinel Troctolite and Anorthosite in Apollo 16 Samples

Abstract. *A spinel troctolite and an anorthosite from the Apollo 16 landing site represent contrasting types of "primitive" lunar cumulates. The two rock types probably formed from the same parent magma type, a high-alumina magnesian basalt, with the troctolite forming earlier by crystal settling, and the anorthosite later, possibly by flotation.*

One of the principal topics of discussion in lunar petrogenesis has been the possibility of early, large-scale differentiation and the importance of cumulate-type rocks. We report here on two Apollo 16 rocks recovered from the lunar highlands which probably represent contrasting types of "primitive" lunar cumulates. Rock 67435 (polished thin sections 67435,14 and 67435,16) is a microbreccia containing a large (4 by 4.5 mm) lithic fragment of spinel troctolite. Rock 62275 (polished thin section 62275,4) is a shock-brecciated anorthosite.

The spinel troctolite lithic fragment in section 67435,14 is an ultramafic rock with a cumulate texture (Fig. 1). The cumulus phases are subhedral to euhedral olivine and pink spinel poikilitically included in plagioclase. The grain size is variable, with spinel ranging from 0.1 to 0.7 mm and olivine from 0.2 to 1.1 mm; the poikilitic plagioclase is much coarser, ranging from 2 to 3 mm. Spinel is unevenly distributed and sometimes occurs in clusters (Fig. 1). The only other phases present are minor Fe-Ni-Co metal grains ranging from minute specks to 0.1 mm in diameter, and fine veinlets of troilite. No pyroxene was found. Spinel and olivine were the first phases to crystallize, with some spinel probably preceding the olivine; these were followed by plagioclase. The mode is given in Table 1 and indicates a high abundance of olivine. However, because of the coarseness of the grain size relative to the size of the fragment the mode may not be representative of the entire rock.

The rock has been mildly shocked, as indicated by the presence of fracture zones with finely recrystallized min-
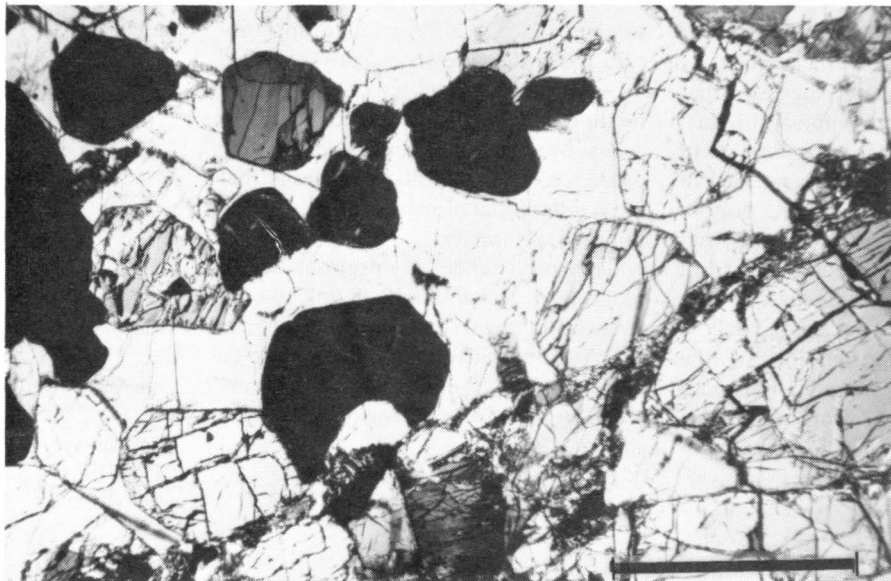

Fig. 1. Photomicrograph, with crossed polarizers, of a portion of the spinel troctolite lithic fragment in Apollo 16 microbreccia 67435,14. Subhedral crystals of spinel (black, in the center) and subhedral olivine (light to dark, in high relief) are poikilitically enclosed within a large single crystal of plagioclase (white). A fracture zone, with recrystallized minerals, crosses the fragment (right center to bottom center of the photograph). Scale bar, 0.5 mm.

erals (one such zone is shown in Fig. 1). Other indications of shock are the presence of mosaic patterns of optical extinction of some olivine and portions of some feldspar grains, as well as the fine veinlets of troilite.

Compositions of minerals were determined with an Applied Research Laboratories EMX-SM electron microprobe by using methods described by Keil (1). The spinel is enriched in $MgAl_2O_4$ (85 mole percent; Table 1). This analysis is typical of other spinel in this rock (2), with a few grains differing slightly. The olivine is highly magnesian (Table 1); analyses of ten crystals give a range of 91.9 to 92.4 mole percent forsterite ($Fo_{91.9}$–$Fo_{92.4}$). This olivine is among the most magnesian reported from the moon; minor occurrences with values near this were found in Apollo 14 and Apollo 15 samples (3). The plagioclase is highly calcic (Table 1); analyses of ten crystals give a range of 96.6 to 97.4 mole percent anorthite ($An_{96.6}$–$An_{97.4}$). In the plagioclase, the concentration of FeO is low (0.16 percent) and that of MgO high (0.65 percent), reflecting the bulk chemistry of the rock. The Fe-Ni-Co grains are remarkably high in Ni (Table 1). The troilite is too small to be analyzed.

A bulk analysis of the spinel troctolite fragment by the broad beam electron microprobe technique (4), is given in Table 1. The high concentrations of MgO (33.7 percent) and Al_2O_3 (15.9 percent) reflect the abundant magnesian olivine and spinel. Even if the rock generally contains a greater amount of plagioclase than is present in this fragment, the magnesian nature of the mineral assemblage would still result in a highly magnesian rock.

The spinel troctolite is embedded in a dense, highly annealed microbreccia consisting of major amounts of plagioclase, minor amounts of olivine and orthopyroxene, and traces of clinopyroxene, Fe-Ni-Co, and troilite. The plagioclase ranges in composition from $An_{93.0}$ to $An_{97.2}$ with one large oval grain being $An_{65.8}$. The olivine ranges from $Fo_{73.9}$ to $Fo_{81.5}$, with a few grains being more magnesian; one grain is of special note in having a $Fo_{95.0}$ composition. The orthopyroxene has a limited range with an average composition of $En_{78.4}$. One grain of clinopyroxene, found in an anorthosite fragment, has a composition of 39.9 mole percent wollastonite, 43.1 enstatite, and 17.0 ferrosilite. Electron microprobe bulk analyses of three

chips of the microbreccia showed their compositional similarity to one another; the average of the analyses is given in Table 1.

The microbreccia is polymict in that it includes the spinel troctolite, as well as minor anorthositic and troctolitic fragments. However, the limited compositional range of the minerals indicates that only a few rock types, of the anorthositic-noritic-troctolitic (ANT) group (5), are included.

Rock 62275 is a brecciated, shock-metamorphosed anorthosite. In thin section it consists of isolated transparent fragments, most of which are fractured, in a finely brecciated matrix. Most of the large transparent frag-

ments are not feldspar, but brownish glass of near-feldspar composition. Only about one-third of the feldspathic fragments are crystalline plagioclase. The glass is not thetomorphic, as indicated by its contents of FeO and MgO, but must have been produced by melting of both plagioclase and mafics. Smaller fragments of olivine, pyroxene, and spinel are present in minor quantities. Our best estimate of the mode, including feldspathic glass with plagioclase, is given in Table 2.

A bulk analysis of this rock is also shown in Table 2. The anorthositic character of this rock is reflected in the high Al_2O_3 (33.1 percent) and CaO

Table 1. Bulk analysis and representative mineralogical data for the spinel troctolite lithic fragment and microbreccia from Apollo 16 sample 67435,14. Ten grains of Fe-Ni-Co were analyzed. The results of the bulk analysis of the troctolite fragment were recalculated to 100 percent by weight; all data are percent by weight. The modal analysis for the troctolite fragment (in percent by volume) is: spinel (5), olivine (69), plagioclase (26), Fe-Ni-Co (trace), and troilite (trace). The molecular proportions (mole percent) are: for plagioclase, anorthite (97.3), albite (2.4), orthoclase (0.3); for olivine, forsterite (92.4), fayalite (7.6); and for spinel, spinel (84.9), hercynite (7.0), chromite (7.9), ulvospinel (0.2); nd, not determined.

Constituent	Bulk analysis	Plagioclase	Olivine	Spinel	Fe-Ni-Co	Microbreccia
SiO_2	37.5	44.4	41.2	0.25		45.4
TiO_2	0.05	0.02	0.03	0.10		0.89
Al_2O_3	15.9	35.7	0.38	62.9		24.1
Cr_2O_3	0.49	nd	0.01	7.9		0.12
FeO	5.8	0.16	7.5	6.9		6.1
MnO	0.16	0.03	0.08	0.03		0.17
MgO	33.7	0.65	51.3	22.5		9.6
CaO	6.2	19.4	0.24	0.22		13.2
Na_2O	0.14	0.27	nd	nd		0.53
K_2O	0.04	0.05	nd	nd		0.23
P_2O_5	0.02	nd	nd	nd		0.17
Totals	100.00	100.68	100.74	100.80		100.51
Fe					47.0–70.4	
Ni					26.7–50.8	
Co					0.64–1.26	

Table 2. Bulk analysis and representative mineralogical data for Apollo 16 anorthosite 62275,4. The results of the bulk analysis were recalculated to 100 percent by weight; all data are percent by weight. The modal analysis (percent by volume) is: feldspathic glass and plagioclase (93), olivine (6), orthopyroxene (1), clinopyroxene (trace), spinel (trace). The molecular proportions (mole percent) are: for plagioclase, anorthite (98.8), albite (1.2); for olivine, forsterite (59.8), fayalite (40.2); for clinopyroxene, wollastonite (45.1), enstatite (38.1), ferrosilite (16.8); for orthopyroxene, wollastonite (3.1), enstatite (67.0), ferrosilite (29.9); and for spinel, chromite (59.3), hercynite (21.5), spinel (12.0), ulvospinel (7.2); nd, not determined.

Constituent	Bulk analysis	Plagioclase	Feldspathic glass	Olivine	Clinopyroxene	Orthopyroxene	Spinel
SiO_2	43.7	43.4	44.3	35.2	51.4	53.5	0.58
TiO_2	0.04	nd	0.13	<0.01	0.46	0.16	2.73
Al_2O_3	33.1	36.2	30.2	0.65	1.43	1.38	16.2
Cr_2O_3	0.29	nd	0.06	0.03	0.24	0.10	42.0
FeO	2.20	0.10	3.4	34.2	10.4	18.8	31.5
MnO	<0.01	nd	0.04	0.42	0.30	0.39	0.24
MgO	1.91	<0.02	3.1	28.5	13.2	23.7	3.5
CaO	18.4	20.3	18.6	0.43	21.7	1.51	0.57
Na_2O	0.30	0.13	0.34	nd	0.07	<0.01	nd
K_2O	0.06	<0.01	0.03	nd	nd	nd	nd
Totals	100.00	100.13	100.20	99.43	99.20	99.54	98.23*

* The total includes 0.86 weight percent V_2O_3.

(18.4 percent) contents. The low FeO and MgO contents reflect the low abundance of mafics. The plagioclase ranges from $An_{97.1}$ to $An_{99.0}$; MgO in the plagioclase is below detection, in contrast with the high MgO content in the plagioclase of the spinel troctolite. The feldspathic glass has an Al_2O_3 content too low for plagioclase, and its FeO (0.1 to 4.1 percent) and MgO (0.10 to 3.3 percent) contents are higher than those found in lunar plagioclase. The olivine grains are small, ranging from minute specks to 0.2 mm; compositionally they are in the range $Fo_{59.0}$ to $Fo_{61.4}$ (Table 2). Orthopyroxene is a minor phase and clinopyroxene is very rare; the grains are found as small discrete crystals. The orthopyroxene ranges from $En_{54.6}$ to $En_{69.8}$ (Table 2). The clinopyroxene has a very limited range and the analysis in Table 2 is typical; compositionally it is transitional between augite and salite. Spinel is a rare constituent, and only two grains large enough to analyze were found. The analysis given in Table 2 shows that it is enriched in $FeCr_2O_4$.

The spinel troctolite described here confirms earlier suggestions (4) that troctolite is a lunar igneous rock type. It is the best example to date of a cumulate texture in a "primitive" rock. Cumulate textures noted previously in lunar igneous rocks, especially in Apollo 12 samples, are in rocks that appear to be related to mare basalts. A lunar spinel troctolite assemblage was first reported as a fragment in an Apollo 11 microbreccia (6), and other troctolitic lithic fragments were described in the same samples (4). An olivine-plagioclase (troctolite) lithic fragment was found in an Apollo 12 sample, but with no spinel (7), and rare spinel troctolite fragments were found in Apollo 14 samples (8, 9). When a spinel phase is present in these troctolites it is enriched in $MgAl_2O_4$. In addition, olivine is rather magnesian (Fo_{74}–Fo_{88}), plagioclase is highly calcic (An_{94}–An_{98}), and no pyroxene or ilmenite is found.

Lunar anorthosites differ from the troctolites, not only in containing more plagioclase, but in the nature of the mafic minerals. Anorthosites usually contain pyroxene, whereas spinel troctolites do not. When spinel is found in anorthosites it is enriched in $FeCr_2O_4$, as shown in Apollo 11 and Apollo 12 fragments (7, 10), and in an Apollo 15 rake sample specimen very similar to 15415 (Genesis Rock) (11). Olivine is usually relatively iron-rich, and opaque phases present in anorthosites include ilmenite, armalcolite, troilite, and metallic Fe-Ni.

The data reported in the literature and the results of the present study indicate that there are essential mineralogical differences between spinel troctolite and anorthosite, which are suggestive of genetic relationships between the two. Such genetic relations may be inferred from a consideration of the system diopside-forsterite-anorthite (12), which offers a first approximation to the parent magmas of these rocks. A $MgAl_2O_4$ spinel field is present on the liquidus of the system on and near the forsterite-anorthite join, and certain liquids in this vicinity would crystallize spinel as one of the earliest phases. On cooling, the liquid would move toward the diopside field with spinel reacting with the liquid to form olivine and plagioclase, unless it is removed by settling, or armored by other crystals. Although $MgAl_2O_4$ spinel is thus removed from later liquids in this differentiation process, the presence of some FeO and Cr_2O_3 in the liquid would probably allow spinel rich in $FeCr_2O_4$ to remain in coexistence with the forsterite-anorthite-diopside (anorthosite) assemblage. The higher Fe/Mg ratios of mafics as well as the presence of ilmenite and armalcolite in anorthosites is also indicative of their formation at a lower temperature, compared to spinel troctolite assemblages.

Thus, if the two rock groups formed from the same parent magma type, the spinel troctolite must have formed early in the differentiation sequence as the result of crystal settling in the melt, whereas the anorthosite must have formed as a later cumulate, possibly by flotation. A similar suggestion has also been made by Roedder and Weiblen (9). It appears that the parent magma must have been a high-alumina magnesian basalt melt.

Martin Prinz
Eric Dowty
Klaus Keil

Department of Geology and *Institute of Meteoritics, University of New Mexico, Albuquerque 87106*

T. E. Bunch

Space Sciences Division, NASA Ames Research Center, Moffett Field, California 94035

References and Notes

1. K. Keil, *Fortschr. Mineral.* 44, 4 (1967).
2. Complete results of the electron microprobe analyses, including structural formulas and molecular components, of all analyzed minerals discussed in the report may be obtained from the authors.
3. The unpublished data include olivine with Fo_{90} in a dunitic fragment in an Apollo 14 microbreccia and in a plagioclase-rich troctolite in the Apollo 15 rake samples.
4. M. Prinz, T. E. Bunch, K. Keil, *Contrib. Mineral. Petrol.* 32, 211 (1971).
5. K. Keil, G. Kurat, M. Prinz, J. A. Green, *Earth Planet. Sci. Lett.* 13, 243 (1972); G. Kurat, K. Keil, M. Prinz, C. E. Nehru, "Proceedings of the Third Lunar Science Conference," *Geochim. Cosmochim. Acta* 1 (Suppl. 3), 707 (1972).
6. K. Keil, T. E. Bunch, M. Prinz, "Proceedings of the Apollo 11 Lunar Science Conference," *Geochim. Cosmochim. Acta* 1 (Suppl. 1), 561 (1970).
7. J. A. Wood, U. B. Marvin, J. B. Reid, G. J. Taylor, J. F. Bower, B. N. Powell, J. S. Dickey, *Smithson. Astrophys. Obs. Spec. Rep.* (1971), p. 333.
8. I. M. Steele, *Earth Planet. Sci. Lett.* 14, 190 (1972); G. M. Brown, C. H. Emeleus, J. G. Holland, A. Peckett, R. Phillips, *Third Lunar Science Conference Abstracts* (Lunar Science Institute, Houston, 1972), p. 95.
9. E. Roedder, P. W. Weiblen, *Earth Planet. Sci. Lett.* 5, 376 (1972).
10. J. A. Wood, U. B. Marvin, B. N. Powell, J. S. Dickey, *Smithson. Astrophys. Obs. Spec. Rep.* (1970), p. 307.
11. E. Dowty, K. Keil, M. Prinz, *The Apollo 15 Lunar Samples* (Lunar Science Institute, Houston, 1972), p. 62.
12. E. F. Osborn and D. B. Tait, *Amer. J. Sci.* (Bowen volume), 413 (1952).
13. We greatly appreciate the assistance of J. A. Green and P. H. Hlava in the electron microprobe work. Supported by NASA grant NGL 32-004-063.

21 August 1972

Breccias from the Lunar Highlands: Preliminary Petrographic Report on Apollo 16 Samples 60017 and 63335

Abstract. Lunar samples 60017,4 and 63335,14 are composed of microbreccias and devitrified glass. These components are predominantly anorthositic, with the exception of a cryptocrystalline clast found in the microbreccia portion of 63335,14 which contains 2.7 percent potassium oxide and 66.7 percent silicon dioxide. The samples have been subjected to extreme shock and thermal metamorphism. The parent materials of the microbreccias include both a coarse-grained anorthosite and a fine-grained subophitic anorthositic gabbro.

Breccia 63335 was collected from Shadow Rock, a 5-m boulder at station 13 on the Cayley Plains of the lunar highlands. The collection site of 60017 is known with less certainty, although it too was probably collected from Shadow Rock (*1*). Thin sections 60017,4 and 63335,14 (shown in Fig. 1, a and b) were studied by using the petrographic microscope and the electron microprobe. Although no complete mineral analyses are presented in this paper, they are available from the authors on request.

60017. Sample 60017,4 consists of two distinct lithologies. One corner of the section (Fig. 1a) consists of a light gray devitrified anorthositic glass, while the rest of the section consists of a darker gray microbreccia. It is impossible to determine from this particular thin section whether either of these lithologies is incorporated within the other.

The devitrified anorthositic glass contains variolitic plagioclase with 93 to 95 mole percent anorthite (An_{93-95}), which decreases in grain size from the outer edge of the section inward toward the contact with the microbreccia. In addition, the glass contains interstitial olivine with 68 mole percent forsterite (Fo_{68}), ilmenite, and metallic iron.

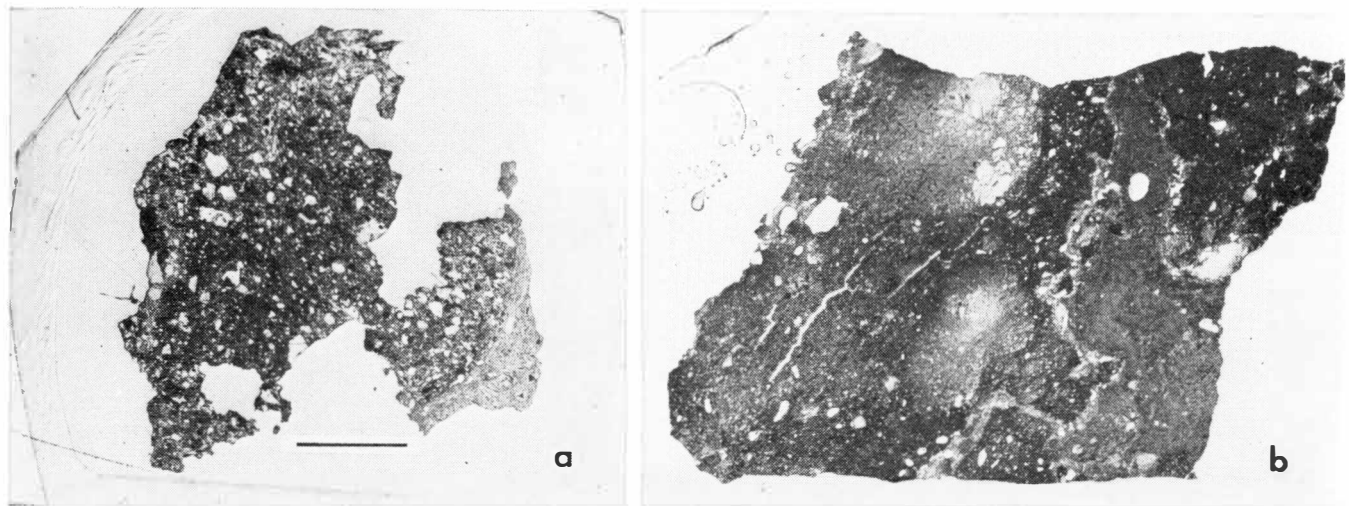The microbreccia is composed primarily of well-rounded anorthositic gabbro clasts, mosaically recrystallized

Fig. 1. (a) Photomicrograph of sample 60017,4. The section consists primarily of microbreccia with an area of devitrified anorthositic glass in the lower right corner. Scale bar, 2.5 mm. (b) Photomicrograph of sample 63335,14 [same scale as (a)]. The section consists primarily of microbreccia, which is transected from top to lower right by a vein of devitrified anorthositic glass. The recrystallized nature of the microbreccia matrix is most readily apparent in the upper left.

anorthosite clasts (possibly devitrified diaplectic glass), and rare crystal clasts, largely olivine, set in a cryptocrystalline matrix. The bulk composition of the matrix, based on defocused beam analyses, is that of gabbroic anorthosite (Table 1, A). A least-squares mixing calculation (2) provides an excellent fit for the bulk chemical composition of the microbreccia matrix with a mixture of 35 percent of the anorthositic gabbro clasts (Table 1, B) and 65 percent of the recrystallized anorthosite fragments (An$_{94-96}$) found in sample 60017.

The anorthositic gabbro clasts in-cluded in the microbreccia are well rounded, subophitic in texture (Fig. 2), and reach a maximum diameter of about 300 μm. Frequently they have a thin rim, which is fine grained and dark in color and is clearly the product of reaction of the clasts with the matrix (Fig. 2). The clasts are composed primarily of small (5 by 20 μm) plagioclase laths (An$_{95}$), interstitial olivine (Fo$_{62-74}$), and fine-grained mesostasis. Accessory minerals include ilmenite, iron metal, and troilite. Fifty ferromagnesian grains from the anorthositic gabbro clasts were analyzed in the course of this investigation, and no pyroxenes were found. Hence, if pyroxene is present, it is extremely fine grained (less than 2 μm).

The average bulk composition of the anorthositic gabbro clasts is given in Table 1, B, along with the compositions of an Apollo 12 mare type basalt (3), a Fra Mauro type basalt (4), the proposed "highland basalt" of Reid et al. (5), anorthosite 15415 (6), and gabbroic anorthosite 15418 (6) for comparison. The anorthositic gabbro in 60017 is much richer in normative anorthite than the mare basalts, and

Table 1. Compositions of Apollo 16 samples 60017 and 63335 and of other lunar materials. Samples 60017 and 63335 were analyzed by defocused beam microprobe; all compositions are given as percent by weight. The samples are: (A) Matrix of the microbreccia in 60017 (average of eight 50-μm spots); (B) gabbroic anorthosite clasts from the microbreccia in 60017 (average of 19 50-μm spots); (C) matrix of the microbreccia in 63335 (average of six 50-μm spots); (D) spherulitic devitrified glass in 63335 (average of two 50-μm spots); (E) Apollo 12 mare basalt (4); (F) Fra Mauro basalt (5); (G) proposed highland basalt (6); (H) anorthosite 15415 (8); (I) gabbroic anorthosite 15418 (8); (J) cryptocrystalline portion of potassium-rich clast from the microbreccia in 60017 (average of six 20-μm spots) (includes 2.4 percent corundum).

Component	A	B	C	D	E	F	G	H	I	J
SiO$_2$	45.69	45.94	45.63	46.23	45.0	46.82	44.35	44.08	44.97	66.71
TiO$_2$	0.22	1.07	1.34	1.38	2.9	2.33	0.43	0.02	0.27	0.09
Al$_2$O$_3$	31.16	22.92	26.91	30.60	8.6	13.81	27.96	35.49	26.73	19.61
FeO	3.26	9.17	6.66	3.43	21.0	15.92	5.05	0.23	5.37	0.29
MgO	2.39	6.37	3.10	1.46	11.6	6.30	6.86	0.09	5.38	0.07
CaO	17.42	14.03	15.43	17.18	9.4	11.57	15.64	19.68	16.10	5.77
Na$_2$O	0.03	0.76	0.83	0.75	0.2	0.80	0.19	0.34	0.31	2.49
K$_2$O	0.43	0.05	0.10	0.08	Trace	0.25	0.01	< 0.01	0.03	2.74
P$_2$O$_5$	0.02	0.06	0.06	0.04		0.25		0.01	0.03	
Total	100.62	100.37	100.06	101.2	99.3	98.52	100.57	99.95	99.37	97.75
Molecular (one cation) norms										
Apatite	< 0.1	0.1	0.1	0.1		0.6		< 0.1	0.1	
Ilmenite	0.3	1.5	1.8	1.9	4.2	3.4	0.6	< 0.1	0.4	0.1
Orthoclase	0.2	0.3	0.6	0.5		1.6	0.1	0.1	0.2	16.7
Albite	3.8	6.9	7.6	6.7	1.9	7.5	1.7	3.1	2.8	23.1
Anorthite	82.7	59.2	70.1	79.6	23.6	34.8	74.5	95.3	72.1	29.5
Quartz	0.4			1.8		0.8		0.1		27.8
Wollastonite	1.3	4.1	2.7	2.0	10.1	9.6	0.9	0.9	3.3	
Enstatite	6.6	11.8	8.3	4.0	26.2	18.3	8.2	0.2	10.3	0.2
Ferrosilite	4.7	8.5	8.2	3.4	22.9	22.3	3.1	0.3	5.5	0.3
Forsterite		4.4	0.3		5.5		7.9		3.5	
Fayalite		3.2	0.3		4.8		3.0		1.9	

more closely resembles the proposed highland basalt and the gabbroic anorthosite 15418. In the report of the Preliminary Examination Team (PET) on the Apollo 16 rocks (7), rock 60017 has been classified as a type 4 rock: a partially molten breccia. It has been suggested that the anorthositic gabbro clasts may be a product of partial melting (8). Although origin by partial melting remains a possibility, we feel that the discrete nature of the areas of anorthositic gabbro favors a clastic origin for this material in 60017,4.

Virtually all the anorthosite clasts contained within the microbreccia exhibit mosaic recrystallization, indicating that they have been subjected to severe shock metamorphism (9). The presence of unshocked plagioclase in the anorthositic gabbro clasts, which are also contained within the microbreccia, implies that the mosaic anorthosite clasts must have been shocked before their incorporation in the microbreccia. It is impossible to determine whether the mosaically recrystallized anorthosite clasts were originally single plagioclase grains or polycrystalline fragments. These anorthosite clasts, which appear as light gray patches in the dark microbreccia in Figs. 1a and 2, show no significant variation in composition (An_{94-96}) either within individual clasts or from one clast to another. Usually the boundaries of the anorthosite clasts are well defined. However, some of the clast boundaries are very indistinct, and the clasts appear to grade into the matrix. In some cases, small fragments of anorthositic gabbro are partially enclosed in the mosaically recrystallized anorthosite clasts. A possible explanation of these textural relationships is that some of the anorthosite "clasts" may have grown during an episode of thermal metamorphism, and that some of the metamorphic overgrowths may have partially surrounded the anorthositic gabbro clasts.

63335. The bulk of the thin section 63335,14 consists of a dark gray microbreccia, which is cut by a vein of light gray devitrified glass. The microbreccia, comprising about 75 percent of the section, contains several types of clasts, including anorthosite, plagioclase, and gabbroic anorthosite. It also contains a few small (less than 30 μm) fragments of olivine, ilmenite, troilite, and iron metal, all of which are set in a cryptocrystalline matrix. The proportion of matrix to crystal and lithic clasts is very high (about 80 percent). The bulk composition of the matrix (Table 1,

C) is that of a gabbroic anorthosite. This composition is similar to that given in the PET report for a 250-mg sample of the same rock [table 1 in (7)].

Dark dendritic laths about 30 μm in width (see the upper left portion of Fig. 1b) appear to have crystallized from the matrix. The crystals have a high index of refraction, and are probably olivine or pyroxene, but the dendritic arms are too fine to permit probe analysis or optical identification. The growth of these dendritic crystals indicates that the microbreccia underwent an episode of extreme thermal metamorphism.

Two large, coarse-grained (1 to 2 mm) anorthosite clasts (An_{93-97}) are included within the microbreccia. They are located in the centers of the top and right edges of the section (Fig. 1b). Although they appear slightly shocked, these clasts do not show the extreme mosaic recrystallization displayed by the anorthosite clasts in 60017. The anorthosite clasts in 63335 are heavily fractured, and appear to have been abraded at their margins, with seams of microbreccia matrix frequently separating the broken fragments. The presence of large anorthite fragments within these clasts indicates that a coarse-grained anorthosite was among the parent materials of microbreccia 63335.

A single clast of gabbroic anorthosite (located just to the left of the anorthosite fragment along the right edge of the thin section, Fig. 1b) is included within the microbreccia portion of 63335. The clast is granular in texture, consisting of equant grains of anorthite
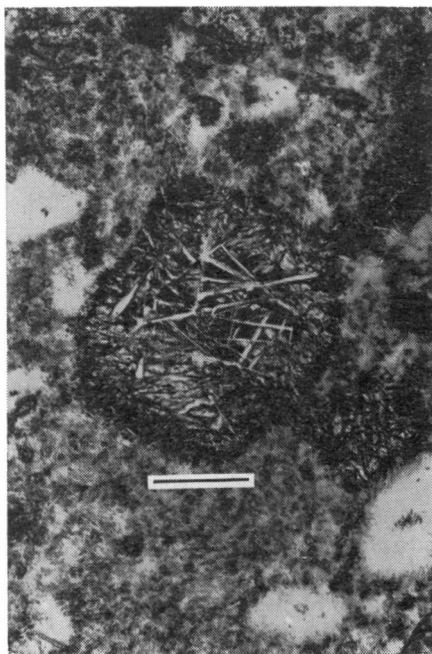
Fig. 2. Photomicrograph of a gabbroic anorthosite clast in the microbreccia portion of 60017,4, showing the reaction rim. The white areas are the mosaically recrystallized anorthosite, and the mottled gray areas the cryptocrystalline matrix. Scale bar, 100 μm.

(An_{95}) and normally zoned olivine (Fo_{72-85}).

Numerous small (50 to 100 μm) clasts of plagioclase within the microbreccia appear to have reacted strongly with the matrix. In some cases, the plagioclase fragments are partially embayed, and the embayments filled with cryptocrystalline matrix. In other cases, several neighboring fragments of plagioclase are in optical continuity, even though separated by bands of matrix. The origin of this texture is not clear. It is possible that the matrix selectively replaced portions of the plagioclase grains during the thermal metamorphic event. Perhaps severely shock-damaged domains underwent replacement reaction more readily than less damaged domains within the same grain.

Several plagioclase-rich areas with indistinct boundaries are present in the dark microbreccia of 63335. These areas may represent resorbed clasts, again suggesting severe thermal metamorphism.

A single highly vesicular, largely cryptocrystalline clast, about 400 μm in diameter, which contains 2.7 percent K_2O and 66.7 percent SiO_2 (Table 1, J), is present in the microbreccia portion of 63335,14. This clast contains a 200-μm subhedral grain of silica (polymorph unknown). The cryptocrystalline portion of the clast is richer in K and Si than KREEP (10), but poorer in these elements than the potassium microgranite found in microbreccia 14321 (4) and the granitic component of 12013 (11).

The light gray vein of devitrified glass cutting across the microbreccia portion of 63335,14 (Fig. 1b) is spherulitic near the top of the section and grades to variolitic near the bottom. It is composed primarily of elongate plagioclase laths (An_{95}), with minor interstitial olivine. The bulk composition of the spherulitic portion is that of gabbroic anorthosite (Table 1, D).

Samples 60017,4 and 63335,14 are similar in several respects. Both samples are composed predominantly of microbreccia and devitrified anorthositic glass. The areas of devitrified glass from the two samples are mineralogically very similar and may share a common

origin. The bulk composition of both samples is dominated by normative anorthite. However, there are also significant differences between the two samples. The mosaically recrystallized anorthosite fragments in the microbreccia portion of 60017 appear to have undergone much more severe shock metamorphism than any of the materials in 63335. Both samples have undergone severe thermal metamorphism, but different results (growth of dendritic ferromagnesian crystals and apparent resorption of plagioclase fragments in the case of 63335, and apparent growth of plagioclase in the case of 60017) suggest that the samples were subjected to different thermal metamorphic conditions. The fine-grained subophitic anorthositic gabbro fragments that are present in the microbreccia portion of 60017 are completely absent in 63335. Hence, if the reported sample locations (1) are correct, Shadow Rock is a complex breccia incorporating several lithologically diverse components which have had different shock and thermal metamorphic histories.

Rocks 60017 and 63335 provide samples of a variety of material which has had a complex history of transportation, lithification, and metamorphism. Although the thin sections investigated were only a few square centimeters in area, previous investigations of small breccia samples have uncovered a wide variety of lithic types (4, 11, 12). Therefore, it may be significant that there is little compositional variety in the material observed in these samples. The samples are dominated by calcic plagioclase, and no material resembling the typical mare basalts was found. We conclude that the region of the Apollo 16 landing site is dominated by anorthositic rocks.

S. J. Kridelbaugh
G. A. McKay, D. F. Weill
Center for Volcanology,
University of Oregon, Eugene 97403

References and Notes

1. Apollo Lunar Geology Investigation Team, *Interagency Report: Astrogeology 51* (open-file report, U.S. Geological Survey, Washington, D.C., 1972).
2. W. B. Bryan, L. W. Finger, F. Chayes, *Science* **163**, 926 (1969).
3. R. Brett, P. Butler, Jr., C. Meyer, Jr., A. M. Reid, H. Takeda, R. Williams, *Geochim. Cosmochim. Acta* **1** (Suppl. 2), 301 (1971).
4. R. Grieve, G. McKay, H. Smith, D. Weill, S. McCallum, in *Lunar Science III*, C. Watkins, Ed. (Contribution No. 88, Lunar Science Institute, Houston, Texas, 1972), p. 338.
5. A. M. Reid, J. Warner, W. I. Ridley, R. W. Brown, *Geochim. Cosmochim. Acta*, in press.
6. Apollo 15 Preliminary Examination Team, *Science* **175**, 363 (1972).
7. Apollo 16 Preliminary Examination Team, *ibid.* **179**, 23 (1973).
8. J. Warner, personal communication.
9. N. M. Short, *Icarus* **13**, 383 (1970).
10. C. Meyer, Jr., R. Brett, N. H. Hubbard, D. A. Morrison, D. S. McKay, F. K. Aitken, H. Takeda, E. Schonfeld, *Geochim. Cosmochim. Acta* **1** (Suppl. 2), 393 (1971).
11. M. J. Drake, I. S. McCallum, G. A. McKay, D. F. Weill, *Earth Planet. Sci. Lett.* **9**, 103 (1970).
12. S. J. Kridelbaugh, R. A. F. Grieve, D. F. Weill, in *The Apollo 15 Lunar Samples*, J. Chamberlain and C. Watkins, Eds. (Lunar Science Institute, Houston, 1972), p. 123.
13. We thank A. R. Duncan, whose constructive criticism greatly improved this manuscript. Supported by NASA grants NGL 38-003-022 and NGL 38-003-020.

11 September 1972

Apollo 16 Exploration of Descartes: A Geologic Summary

Abstract. *The Cayley Plains at the Apollo 16 landing site consist of crudely stratified breccias to a depth of at least 200 meters, overlain by a regolith 10 to 15 meters thick. Samples, photographs, and observations by the astronauts indicate that most of the rocks are impact breccias derived from an anorthosite-gabbro complex. The least brecciated members of the suite include coarse-grained anorthosite and finer-grained, more mafic rocks, some with igneous and some with metamorphic textures. Much of the traverse area is covered by ejecta from North Ray and South Ray craters, but the abundance of rock fragments increases to the south toward the younger South Ray crater. The Descartes highlands, a distinct morphologic entity, differ from the adjacent Cayley formation more in physiographic expression than in lithologic character.*

Orion, the lunar module (LM) of Apollo 16, landed at latitude 8°59′29″S and longitude 15°30′52″E at the west edge of the Descartes Mountains. It was about 50 km west of the Kant Plateau, part of the highest topographic surface on the near side of the moon (Figs. 1 and 2). This was the only planned landing in the central lunar highlands. The crew explored and sampled an area characteristic of both cratered terra plains and rugged hilly and furrowed terra, units never before directly sampled. The area is underlain by thick impact breccias rather than the volcanic rocks predicted from photogeologic studies.

The three sorties by vehicle from the LM extended 1.4 km west, 3.7 km south, and 4.4 km north, comprising a total traverse distance of 20.3 km. Ninety-five kg of rocks and soil were collected, 1765 photographs were taken on the surface, and the total time spent outside the LM was 20 hours, 14 minutes. The lunar locations of all samples and the lunar orientations of 45 rocks have been determined.

Geologic studies of the Descartes region began more than 10 years ago with telescopic observations (*1, 2*) and continued with the better resolution of Lunar Orbiter and Apollo photography (*3–6*).

Upland plains-forming units, such as the Cayley formation, cover about 7 percent of the near side of the moon and occupy more area than any other identifiable unit except mare material. Characteristically, they form low-relief plains in the floors of older depressions. Craters with diameters of 300 m to 2 km are abundant on most of the surfaces. Near the landing site the formation is divided into smooth and irregular subunits (*5*), but only the irregular unit occurs within the planned traverse area. A volcanic origin was preferred by most workers (*1–8*), although it was recognized that photogeologic studies could not preclude impact or mass-wasting origins (*1, 6*). Elsewhere, Cayley materials appear to lie on Fra Mauro deposits and, in turn, are covered by mare basalts (*2, 7*).

On the three traverses two distinct morphologic units were investigated, the terra plains mapped as Cayley formation, and the Descartes Mountains or highlands (Fig. 2). Specifically, the study of the Cayley formation was planned to determine the lateral variation of the stratigraphic section between North Ray and South Ray craters (Fig. 3), the petrology of the formation, and the characteristics of the regolith throughout the area. The prime Cayley sampling areas were at the LM and west of it, where Flag and Spook craters would permit sampling to depths of about 60 m. Deeper parts of the Cayley formation, which have been excavated by the larger North Ray and South Ray impacts, were accessible for sampling on the rim of North Ray crater and in
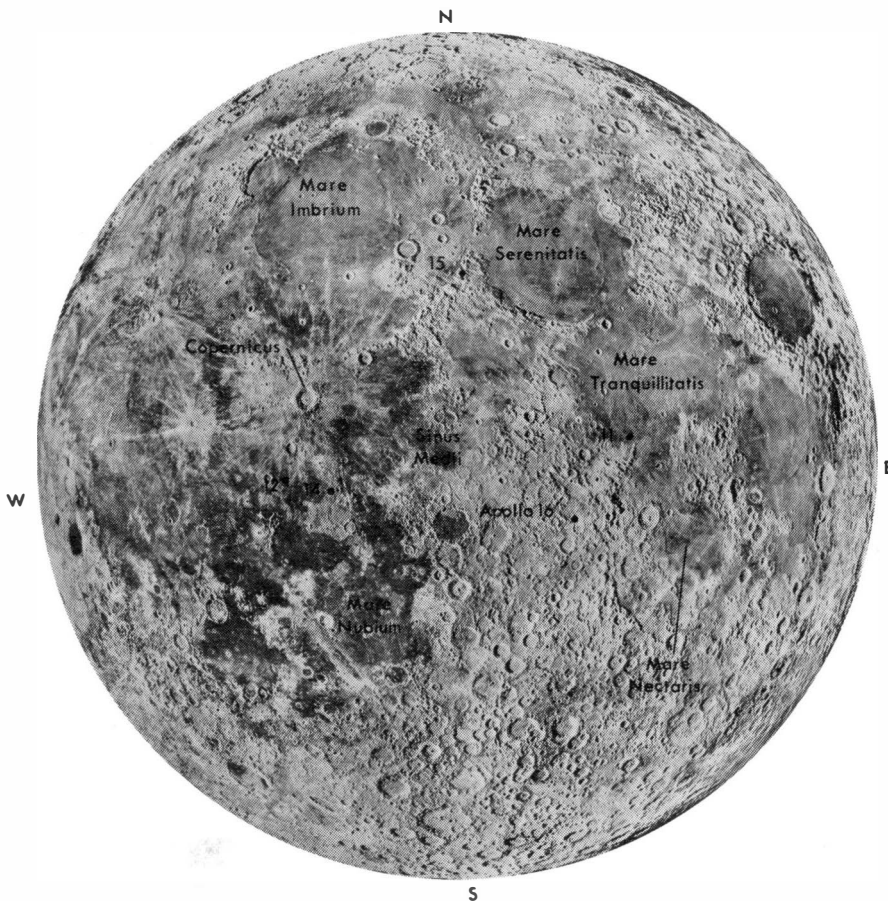

Fig. 1. Composite photograph of the full moon showing the maria surrounding the Apollo 16 central highlands area and the Apollo landing sites to date.

the bright ray deposits of South Ray.

Materials of the Descartes highlands form hilly and mountainous regions that are topographically higher than the Cayley Plains (Fig. 2). The Descartes unit is one of the better examples of rugged terrain that does not appear to be related to craters or multiring basins. Milton (2) pointed out that the unit forms a deposit of considerable thickness, perhaps 1 km, and that its relief is largely intrinsic. Milton (2, 7) and Trask and McCauley (6) interpreted positive landforms in the Descartes highlands as volcanic. The stratigraphic relationships with the adjacent Cayley formation were ambiguous, so that younger, older, and contemporaneous interpretations all were possible. The north flank of Stone Mountain was the principal sampling area for Descartes highland materials (Fig. 3).

The Kant Plateau occupies much of the central region of the Theophilus quadrangle (2) (Fig. 2). Materials of the Kant Plateau were not believed to underlie the Apollo 16 site, but ejecta derived from the plateau might be present in the traverse area. Materials
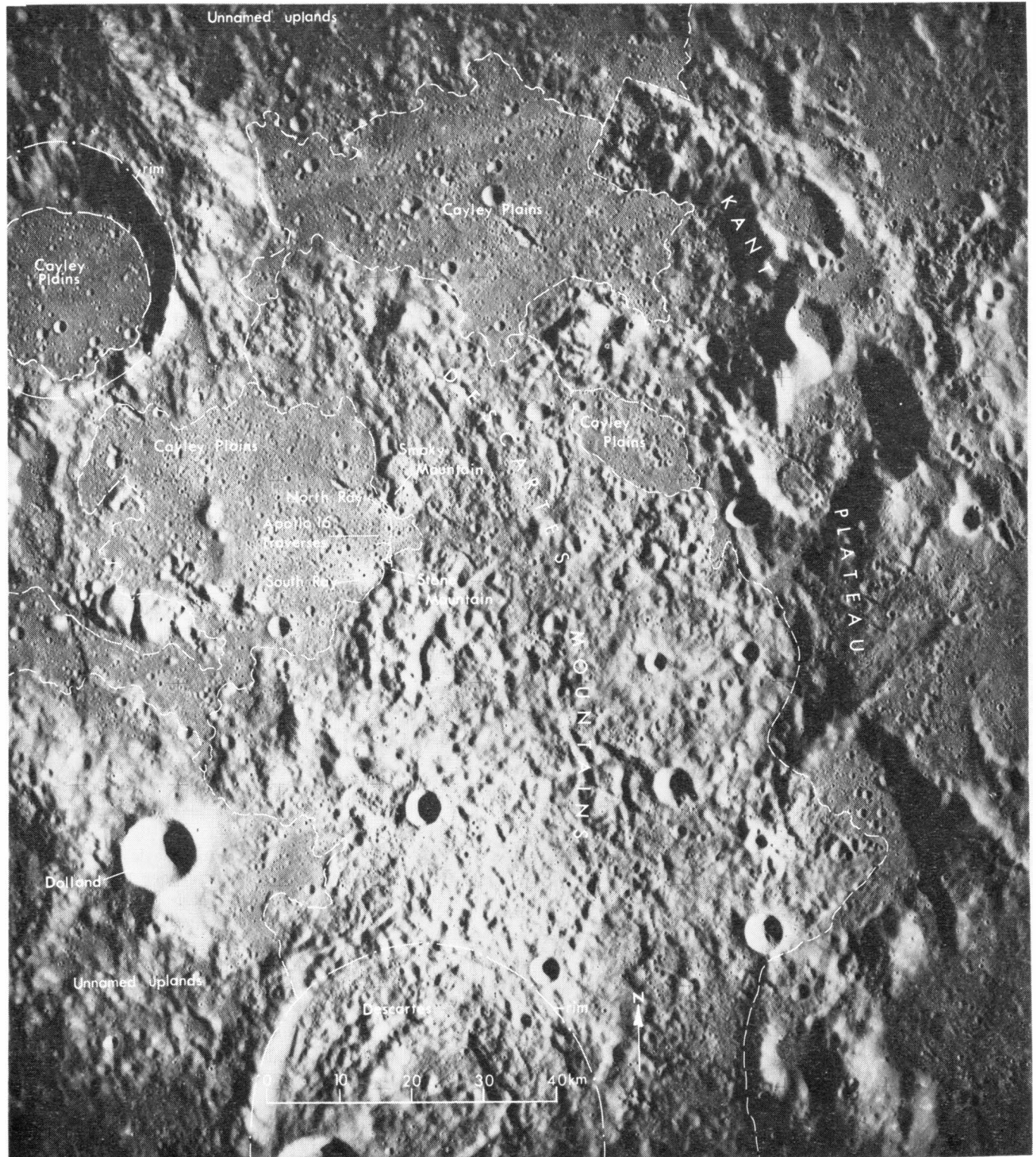

Fig. 2. Apollo 16 landing site, traverse area, and related regional lunar features. [NASA mapping camera photograph M-439]

of the plateau were interpreted by Milton as volcanic, although he noted a lack of distinct volcanic landforms.

Ray materials from North Ray and South Ray craters were shown on premission maps as mantling a considerable part of the traverse area, both on the plains and on the adjacent highlands (4, 5). Impact craters of Imbrian to late-Copernican age were mapped throughout the region. In addition, rimless to low-rimmed elongate
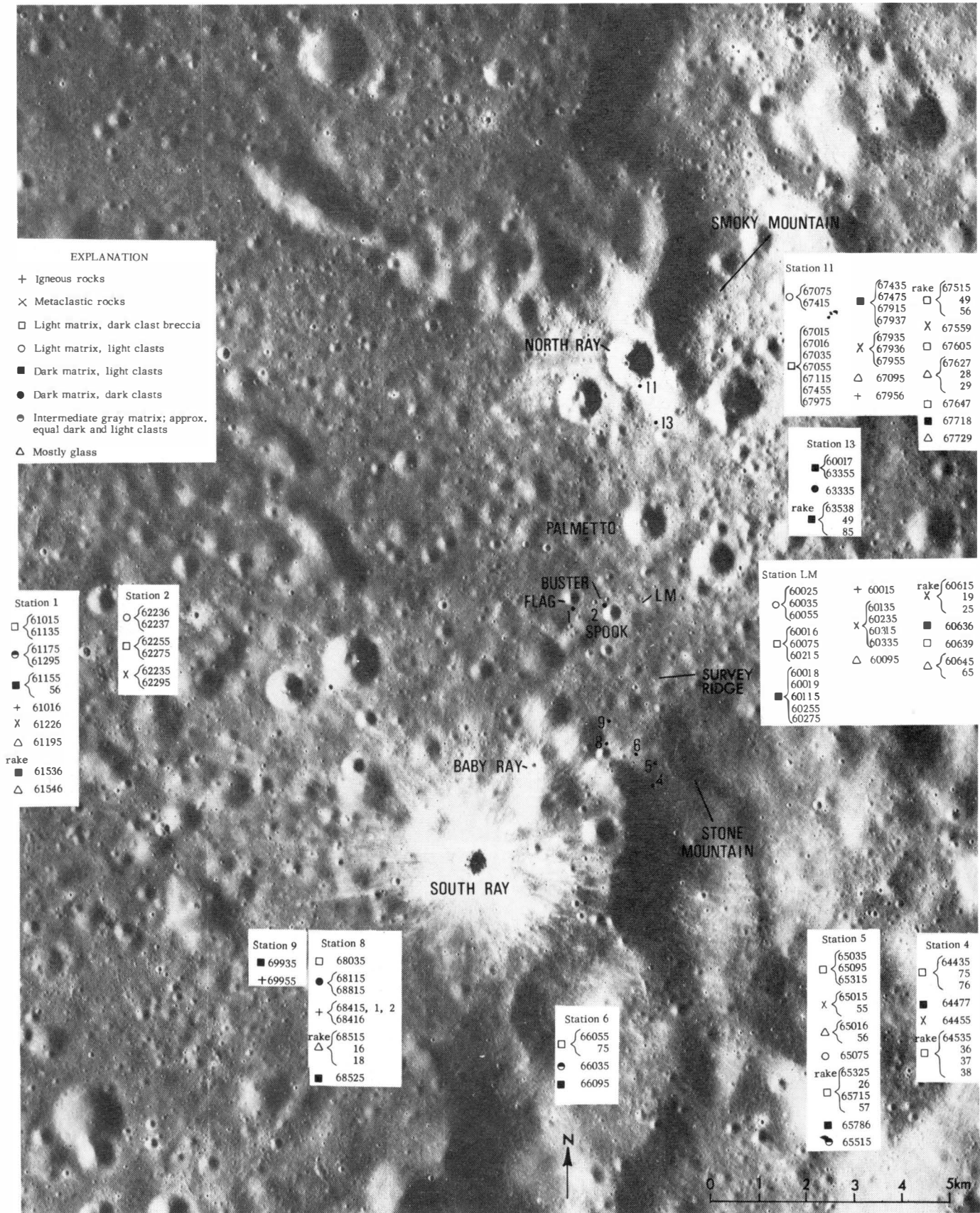

Fig. 3. Apollo 16 traverse stations, craters, and other local landmarks, and the distribution of rock samples larger than 25 g. The preliminary rock classification was based on megascopic observations. [NASA panoramic camera photograph 4623]

depressions that were interpreted as either secondary craters from Theophilus or of internal origin were mapped. The rarity of volcanic rocks observed or sampled suggests that the secondary crater hypothesis is probably the correct one. Topographic benches on the flanks of Stone Mountain, and ledges and albedo bands in the walls of several craters suggest internal layering in some exposed slopes.

Surficial materials. Broad areas of fresh, blocky debris on the surface correspond roughly to the radial ray patterns mapped around North Ray and South Ray craters, the two most apparent sources of surface debris on the Cayley Plains (Fig. 3). The abundance of rock fragments greater than 2 cm across increases progressively from north to south over the entire traverse area (Fig. 4). Typically, fragments greater than 2 cm in the ejecta of North Ray crater cover considerably less than 1 percent of the surface area (Fig. 5a), whereas abundances of as much as about 7 percent are common south of the LM area in rays from South Ray crater (Fig. 5b).

Rays from South Ray crater extend at least 9 to 10 km from the crater into areas west and southeast of North Ray crater. They are superposed on the older North Ray ejecta. South Ray crater ejecta also appear to mantle much of the surface of Stone Mountain in the vicinity of stations 4 and 5 (Fig. 3). The wide extent of these rays greatly increases the possibility that ray material rather than materials derived from local bedrock was sampled at many of the traverse stations. Ejecta from Baby Ray crater overlie those of South Ray and are therefore youngest of all; samples from this smaller and very fresh crater might have been found at stations 8 or 9. The mapped ejecta of North Ray extend shorter distances outward (less than 3 km south into the traverse area) than do those of South Ray, and bright rays are not so prevalent. This apparent difference in distribution presumably is the result of the greater age of North Ray crater and a greater amount of "weathering" of its ejecta.

Rocks exposed on the lunar surface tend to become more rounded, more deeply buried, and more filleted with age. Boulders in the vicinity of South Ray crater and in its mappable rays are more angular than those in the vicinity of North Ray crater. However, the angularity of blocks must be used with caution in distinguishing South Ray from North Ray ejecta when the relative resistance to erosion is not known. By the same reasoning, estimates of relative ages are risky except when rocks of similar strength can be compared. Useful measurements were made, however, on the size-frequency distribution of fragments along the Apollo 16 traverse routes, partly shown in Fig. 4. Most resolvable fragments range in size from 2 to 40 cm; a few are as much as 90 cm in diameter. Larger blocks are present locally, but they are commonly too distant from the camera to be included in the measurements. The most abundant resolvable fragments are in the size class 2 to 5 cm, which typically constitutes 25 to 90 percent of the area covered by fragments. Those in the size class 5 to 10 cm are second in abundance.

On all the Apollo missions it has been difficult to determine the nature of the local bedrock by sampling through a regolith of surficial debris.
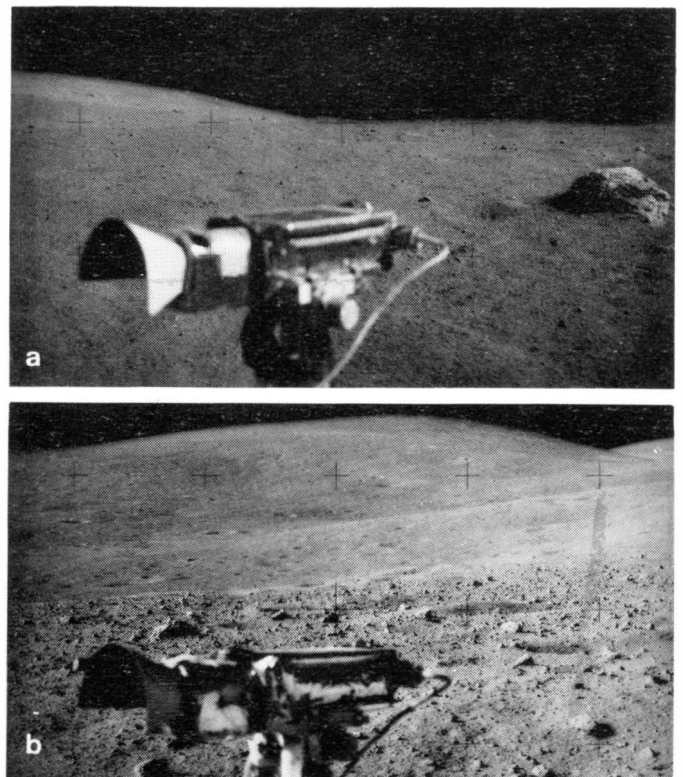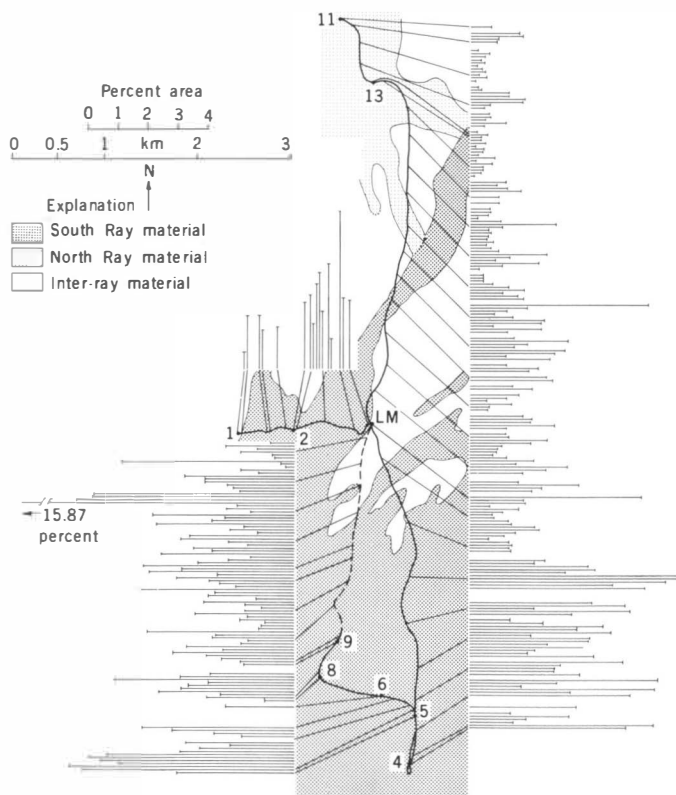

Fig. 4 (left). Frequency distribution of fragments larger than 2 cm counted in 324 surface photographs taken from the vehicle along the Apollo 16 traverse routes. The varying bar lengths represent the percentages (percent area scale) of the area covered by the fragments. The kilometer scale refers to the traverse map, where the lines show the traverse route and the numbers refer to sampling stations.   Fig. 5 (right). (a) Typical fragment population about 1 km southeast of the rim of North Ray crater. Fragments cover 0.2 percent of the surface. The large rock to the right is approximately 2 m in diameter. [NASA photograph AS16-111-18146] (b) Fragment population in the bright ray area (Survey Ridge) about 5 km northeast of South Ray crater. Fragments cover 7 percent of the area. [NASA photograph AS16-110-17895]

a heterogeneous mixture of rocks and soils derived from underlying bedrock or older regolith and contaminated by an unknown amount of ejecta from distant impact events. The Apollo 15 crew found outcrops of mare basalt at the edge of Hadley Rille. The Descartes terrane in the area traversed by Apollo 16 does not contain bedrock protruding through the regolith; therefore, the astronauts had to rely on fresh, blocky crater rims and bright ray deposits to provide samples derived from beneath the regolith. On the basis of the smallest blocky and flat-bottomed craters, the regolith thickness is estimated to be 10 to 15 m over the site. Blocky debris with recognizable planar structures forms a bench about 10 m below the crater rim of Buster crater at station 2 (Fig. 3). This bench is interpreted as local bedrock or possibly an overturned layer of Spook crater rim material; it could, however, be an isolated large block within the regolith.

The bulk chemical compositions of Cayley soils determined by the Preliminary Examination Team (9) show a surprising uniformity throughout the traverse area. The rock compositions show a slightly larger range, but still have remarkably little variation. The rocks are roughly equivalent in composition to anorthosite and anorthositic gabbro. This indicates that the criteria of texture and albedo used in distinguishing the several breccia types probably reflect variations in their history rather than in their source materials (10).

The presence of high-albedo regolith under a darker surface layer at all sample stations, with the possible exception of station 5, suggests that the surface material darkens with time and that the entire thickness of the high-albedo regolith layer was deposited in a single event. Studies of the returned cores should shed light on the time sequence of the layers preserved.

Cayley formation. The Cayley formation has been penetrated by craters to a depth of approximately 200 m at North Ray crater (Fig. 6), to depths of 50 to 60 m west of the LM, and to unknown depths at several localities over a distance of about 4 km between the LM and Stone Mountain. Sampling of South Ray ejecta from its conspicuous rays may have provided both light and dark materials from as deep as 150 m. The light rays near the crater give the highest albedo readings yet measured (55 percent). These are presumably a result of the anorthositic composition of the ejecta, and are measurable with the high resolution of the telephoto camera system. North Ray and South Ray craters have penetrated a topographic range of more than 300 m (Fig. 6); this could represent the stratigraphic range of Cayley samples if essentially horizontal layering is assumed.

Heterogeneous fragmental rocks are the dominant lithology of the Cayley formation at the Apollo 16 site. The rocks closely resemble in texture some samples collected by the Apollo 15 crew from the Apennine front and do not exhibit the extreme multiple brecciation and metamorphism of the Apollo 14 samples. Although several distinctly different rock types are present, breccias with light and dark matrices dominate the surface debris that was sampled and photographed. Significant variations in the proportions of breccia types appear in the ejecta of each major crater sampled, but there do not appear to be any basic differences between the rock assemblages collected from North Ray and South Ray craters.

The few crystalline rocks collected range from anorthosite to feldspar-rich gabbros and include minor amounts of fine-grained, highly feldspathic vuggy
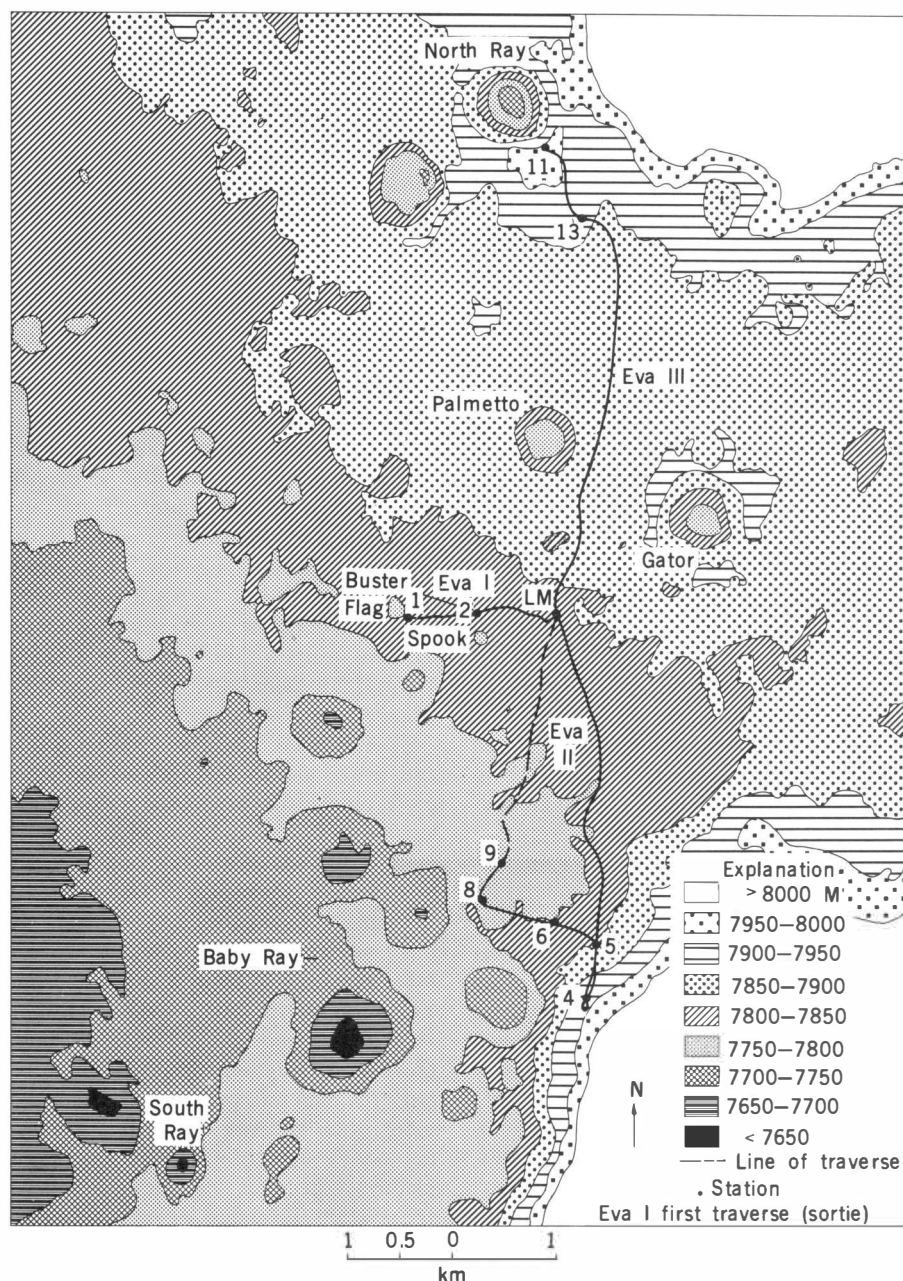

Fig. 6. Hypsographic map of the Apollo 16 landing area showing the regional distribution of topographic zones in 50-m increments. The elevations are from a topographic map of Descartes (*19*). The depth of South Ray crater was modified from postmission photography. The line of traverse is dashed where approximate.

Explanation
> 8000 M
7950–8000
7900–7950
7850–7900
7800–7850
7750–7800
7700–7750
7650–7700
< 7650
— — — Line of traverse
• Station
Eva I first traverse (sortie)

1 0.5 0 1
km

igneous rocks (Fig. 3). These were collected from the ray deposits from South Ray crater, the deepest available source of fresh rocks from the Cayley formation. One rock of this type was collected on North Ray crater; it is of uncertain origin with respect to South Ray crater. The more abundant type of crystalline rock is metamorphic, probably representing recrystallized fragmental rocks composed of similar feldspar-rich materials, and was collected throughout the site. These are the metaclastic rocks of Wilshire *et al.* (*11*). They have also been interpreted as products of contact metamorphism (*9*).

If the igneous rocks represent large clasts within the deepest breccias sampled from beneath the Cayley Plains, then it is reasonable to propose a succession of increasingly fragmented rocks toward the surface that would account for the textural and albedo differences (for example, the glass content) in all the rocks which otherwise may have similar bulk compositions. This model would also explain the combined features of crude local stratification and complex discontinuities within the same crater wall, like those in both South Ray and North Ray craters.

Evidence for layering within the Cayley formation is derived from both the surface photography and the distribution of rock types, as classified by Wilshire *et al.* (*11*) (Fig. 3), and is shown by North Ray and South Ray craters (Figs. 7 and 8 and cover). Our classification scheme differs from that used by the Preliminary Examination Team (*9*): It involves a megascopic division of breccia types according to the pro-portions of light and dark materials in both clasts and matrix, and the assump-tion that both single- and multiple-impact breccias are present and can be separated into classes. If an anortho-sitic complex is the target rock for a major impact, then breccias will be pro-duced in which metaclastic debris or partial melts of the parent material, or both, will constitute a dark matrix surrounding shocked light-colored anortho-site clasts. If this, in turn, is the target rock for a second impact, it will pro-duce clasts derived both from the dark matrix and from the coherent parts of the light clasts. The remaining light anorthosite debris will be mobilized to become the light matrix of a mixed light- and dark-clast breccia. The dif-ferent proportions of clast types will produce striking differences in the ap-pearance of the hand specimens, but
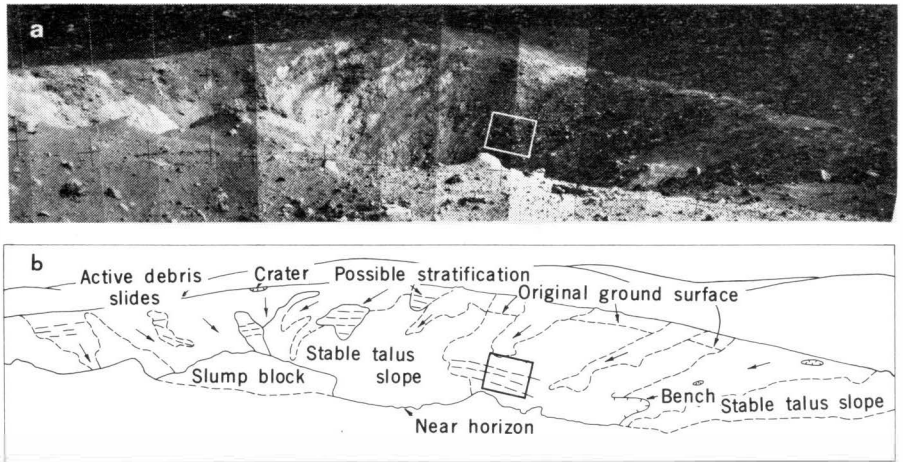

Fig. 7. (a) North Ray crater wall photographed from the southeast rim near station 11. The opposite rim is about 1 km away. House Rock is to the right of the panorama. [NASA photographs AS16-106-17252 to AS16-106-17262] (b) Sketch of features observed in (a). The area marked by the rectangle is the location in the cover picture.

will not appreciably change the bulk chemical composition of the resulting rocks.

The sequence inferred, from bottom to top of the Cayley formation, is as follows:

1) A breccia of anorthositic gabbro and metaclastic crystalline rocks exposed in the lower half of South Ray crater (below the bench in Fig. 8b) and distributed as hard white angular fragments throughout the ray-covered south half of the landing site. This constitutes nearly 25 percent of the fragment population at stations 8 and 9. The metamorphic or metaclastic crystalline rocks are first-cycle or contact-metamorphosed breccias from the upper zone of this body and are distributed as sparse clasts throughout the site.

2) Very coherent breccias with a dark matrix, which are first-generation breccias derived largely from crystalline rocks (*11*). This unit is approximately 30 m thick, above a bench in South Ray crater, and it is apparently also penetrated by Baby Ray crater. It may be correlative with the lowest stratigraphic horizon in North Ray crater, as represented by House rock and Shadow rock, which were sampled by the crew on the North Ray rim at stations 11 and 13. These dark-colored breccias dominate the fragment population on the Cayley Plains in the southern half of the site.

3) A friable and poorly consolidated light-colored stratum 50 to 100 m thick. It is inferred that this unit lies above the dark-matrix rocks (Fig. 8a), and is the source of the fine light "soils" distributed thinly over much of the rim of North Ray crater. It apparently fills

the interstices and thinly covers the blocky ejecta blanket. It may account for the anomalously low proportions of fragments shown in Figs. 4 and 5a.

4) More blocky breccias with a light matrix in the upper 90 to 100 m of North Ray crater wall (cover). The unit appears to be locally stratified as shown by discontinuous linear patterns of coherent blocks in Fig. 7 and the cover picture. These rocks dominate the fragment population of the southeast rim of North Ray crater. They are interpreted by Wilshire *et al.* (*11*) as second-generation breccias. This unit may represent the higher Cayley surface that extends from a scarp about 0.5 km north of the LM to the ridge 50 m high penetrated by North Ray crater (Figs. 3 and 6).

5) Rim materials of an older regolith and mixed debris from the underlying units on North Ray crater rim. This local unit is the overturned flap comprising approximately the upper 30 m of the crater wall (Figs. 7 and 8).

Figure 7 is constructed from one of three sets of photographs taken through a polarizing filter from a single station. The polarimetric data provide additional evidence that only highly shocked breccias, or regolith derived from this type of material, are exposed on the inner walls and rim of North Ray crater; no basalt is identifiable. Telephoto pictures like that on the cover also show that the large blocks are predominantly light-matrix breccias and have a crude planar structure.

In summary, the Cayley formation at the Apollo 16 site appears to be a thick (at least 200 m, possibly more than 300 m), crudely stratified breccia
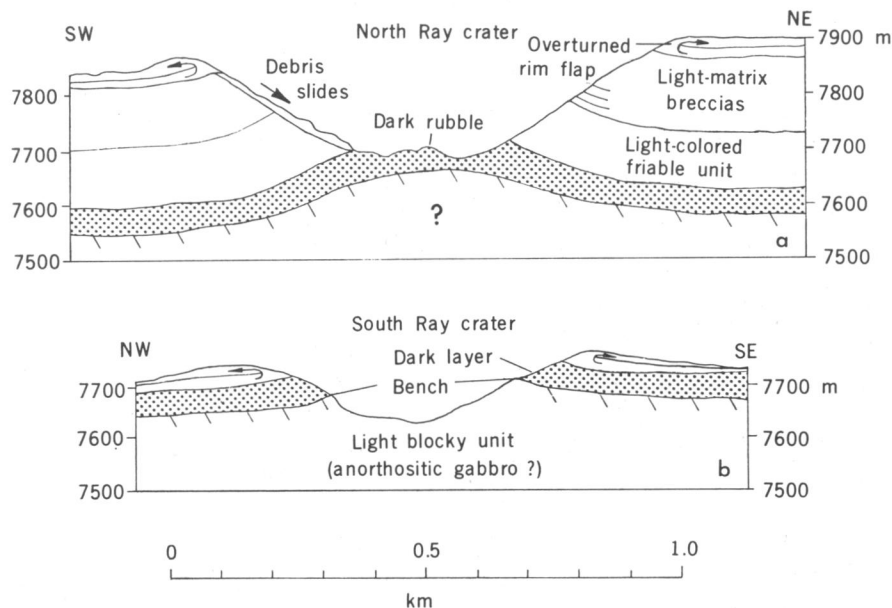
Fig. 8. Schematic geologic cross sections of (a) North Ray and (b) South Ray craters, showing the possible correlation of the dark layer (stippled).

unit whose components are derived from plutonic anorthosite, feldspathic gabbro, and metamorphic rock of similar composition. The elemental composition of the Cayley formation is similar to that observed over large regions of the lunar highlands, as shown by the orbital x-ray experiments of Apollo 15 and Apollo 16 (*12, 13*). The textures and structures of the breccias and the clasts within them resemble those of terrestrial impact breccias. They do not resemble those of volcanic rocks.

Descartes highlands. The materials of the Descartes highlands were the sampling objectives at stations 4 and 5 on Stone Mountain (Figs. 2 and 3). The traverse route in this area is heavily mantled by angular blocky debris, apparently ejected from South Ray crater. The regolith under this blocky material is relatively fine grained, with a few coarse fragments. The crew observed no craters that appear to penetrate bedrock or that expose coarse blocks of underlying materials.

Most of the rock samples collected at stations 4 and 5 on Stone Mountain are light-matrix breccias (Fig. 3). The photographic evidence weighs in favor of a South Ray origin for most of these rocks. However, their similarity to the high concentration of light-matrix breccias at North Ray suggests, as an alternative explanation, that the light-matrix breccias are representative of Stone Mountain as well as the comparably higher elevations on North Ray crater, and thus both may be considered to be true Descartes material.

At station 5, the crew sought and collected a number of more rounded fragments that did not appear to be associated with rays; they were generally from the shielded locations in the crater walls and probably include some Descartes materials, but none has yet been uniquely identified as such.

Seven soil samples, including one double drive tube, were taken at stations 4 and 5. Although variable dilution by South Ray fines is expected, these samples may be dominantly Descartes materials. However, comparisons of these soils with soils from the Cayley Plains (*9*) show marked compositional similarities, adding support to the evidence from the rock collections that the Descartes materials are lithologically similar to the Cayley formation.

The precise nature of the Descartes highlands materials has not yet been established. The available evidence indicates that the Descartes highlands differ from the adjacent Cayley formation more in physiographic expression than in lithologic character. It may be, however, that Descartes material was simply not available for collection at the surface in the traverse area.

Regional relations. If the rocks sampled at this landing site are typical of the upland terra plains and mountainous highlands, then the premare feldspar-rich basalt (*13, 14*) that has been postulated as a stage in lunar evolution (*15*) is no longer a feasible concept. Postmission analysis of the orbital photography has resulted in a series of studies (*16*) pointing to analogs elsewhere on the moon of features in or near the Apollo 16 landing site. Two of these having a direct relationship to the landing site are briefly mentioned here.

Eggleton and Schaber (*17*) present topographic and photogeologic data supporting the hypothesis that the Cayley formation is highly fluidized Imbrium ejecta filling the topographic low areas in the central highlands that surround the Apollo 16 landing site.

Soderblom and Boyce (*18*) determined the ages of nearside and farside terra plains by using the Apollo 16 metric photography. They concluded that all the terra plains studied, including the Cayley Plains of the Apollo 16 landing site, have a narrow range in age and are younger than the Fra Mauro formation, and that the youngest is transitional in age with the oldest mare.

The Apollo 16 results have demonstrated again that the moon is far more complex than predicted on the basis of early studies. The remarkable suite of feldspathic crystalline rocks and breccias from the largest lateral and vertical range sampled to date helps to clarify the origin and history of a significant part of the lunar highlands and make possible more precise statements of new questions.

APOLLO FIELD GEOLOGY
INVESTIGATION TEAM*

References and Notes

1. R. E. Eggleton and C. H. Marshall, in *Astrogeologic Studies Semi-annual Report, February 26, 1961 to August 24, 1961* (open-file report, U.S. Geological Survey, Washington, D.C., 1962), pp. 132–136.
2. D. J. Milton, *Miscellaneous Geological Investigations Map I-546*, scale 1:1,000,000 (U.S. Geological Survey, Washington, D.C., 1968).
3. ——, *Miscellaneous Geological Investigations Map I-748*, scale 1:250,000 (U.S. Geological Survey, Washington, D.C. 1972); D. E. Wilhelms and J. F. McCauley, *Miscellaneous Geological Investigations Map I-703*, scale 1 : 5,000,000 (U.S. Geological Survey, Washington, D.C., 1971); J. W. Head III and A. F. H. Goetz, *J. Geophys. Res.* 77, 1368 (1972).
4. C. A. Hodges, *Miscellaneous Geologic Investigations Map I-748*, scale 1:50,000 (U.S. Geological Survey, Washington, D.C., 1972); D. P. Elston, E. L. Boudette, J. P. Schafer, W. R. Muehlberger, J. P. Sevier, *Geotimes* 17 (No. 3), 27 (1972).
5. D. P. Elston, E. L. Boudette, J. P. Schafer, *Geology of the Apollo 16 Landing Site Area* (open-file report, U.S. Geological Survey, Washington, D.C., 1972).
6. N. J. Trask and J. F. McCauley, *Earth Planet. Sci. Lett.* 14, 201 (1972).
7. D. J. Milton, in *Astrogeologic Studies Annual Progress Report, July 1963–1964* (open-file report, U.S. Geological Survey, Washington, D.C., 1964), part A, pp. 17–27.
8. D. E. Wilhelms, in *Astrogeologic Studies Annual Progress Report, July 1964–July 1965* (open-file report, U.S. Geological Survey, Washington, D.C., 1965), pp. 13–28.

9. Lunar Sample Preliminary Examination Team, *Science* **179**, 23 (1973).
10. J. B. Adams and T. D. McCord, *ibid.* **171**, 567 (1971).
11. H. G. Wilshire, E. D. Jackson, D. Stuart-Alexander, *U.S. Geol. Surv. J. Res.,* in press.
12. I. Adler, J. Trombka, J. Gerard, R. Schmadebeck, P. Lowman, H. Blodgett, L. Yin, E. Eller, R. Lamothe, P. Gorenstein, P. Bjorkholm, B. Harris, H. Gursky, in *Apollo 15 Preliminary Science Report* (NASA SP-289, National Aeronautics and Space Administration, Washington, D.C., 1972), pp. 17-1 to 17-17.
13. I. Adler, J. Trombka, J. Gerard, P. Lowman, R. Schmadebeck, H. Blodgett, E. Eller, L. Yin, R. Lamothe, G. Osswald, P. Gorenstein, P. Bjorkholm, H. Gursky, B. Harris, *Science* **177**, 256 (1972).
14. A. M. Reid, W. I. Ridley, J. Warner, R. S. Harmon, R. Brett, P. Jakes, R. W. Brown, in *Abstracts of the Third Lunar Science Conference* (LSI Contribution 88, Lunar Science Institute, Houston, Texas, 1972), pp. 640–642.
15. J. F. McCauley and D. E. Wilhelms, *Icarus* **15**, 363 (1971).
16. *Apollo 16 Preliminary Science Report* (NASA SP-315, National Aeronautics and Space Administration, Washington, D.C., in press).
17. R. E. Eggleton and G. G. Schaber, in *ibid.*
18. L. A. Soderblom and J. M. Boyce, in *ibid.*
19. "Topographic map of Descartes," scale 1 : 50,000 (U.S. Army Topographic Command, Washington, D.C., March 1972).
20. Work done under NASA contract T-5874A. Publication authorized by the director, U.S. Geological Survey.

Volatile-Rich Lunar Soil: Evidence of Possible Cometary Impact

Abstract. *A subsurface Apollo 16 soil, 61221, is much richer in volatile compounds than soils from any other locations or sites as shown by thermal analysis–gas release measurements. A weight loss of 0.03 percent during the interval 175° to 350°C was associated with the release of water, carbon dioxide, methane, hydrogen cyanide, hydrogen, and minor amounts of hydrocarbons and other species. These volatile components may have been brought to this site by a comet, which may have formed North Ray crater.*

One of the fundamental characteristics of the moon is its low abundance of the volatile elements hydrogen, carbon, nitrogen, and oxygen and their associated low molecular weight compounds and mineral phases (1). Anders (2) noted that the low abundances of other volatiles, such as lead, bismuth, and thallium, are probably associated with the accretional history of the moon. The only exceptions to the consistent depletion of volatile elements and compounds in samples from all lunar sites are the enrichments in the soils and selected breccias of elements derived from the solar wind (such as hydrogen, helium, carbon, and nitrogen) (1, 3). We now report the first occurrence of a volatile-rich subsurface sample derived from North Ray crater (sample 61221). The volatiles in this sample are believed not to be of solar wind origin, but may have arisen from the cometary impact that created North Ray crater.

Apollo 16 soil sample 61221 contains an unusually large amount of low-temperature volatile components. The sample, collected at station 1 near Plum crater by astronaut Duke, was taken at a depth of about 30 to 35 cm beneath the surface (4, 5). It is unusually white in color, much coarser in grain size (median size ranging from 250 to 300 μm compared to 76 to 122 μm for other Apollo 16 soils, exclusive of those from North Ray crater), and distinctly different petrographically from the normal medium-gray surface soil which covered the white soil (6). The sample contains an exceptionally small amount of glass agglutinates (8 percent), in contrast to the darker-colored soil 61241 (greater than 50 percent agglutinates) which covers the subsurface sample [table 3 in (6)]. McKay and co-workers (7) have shown that the percentage of glass agglutinates in a lunar soil provides a relative index of maturity or residence time on the lunar surface; we conclude that the darker upper soil 61241 is a more mature soil than 61221 (6). The grain sizes and abundance of agglutinates in 61221 are similar to those of Apollo 16 soils collected at North Ray crater and station 13 (on the ejecta blanket of North Ray crater) (5, 6). Further evidence of the similarity of soil 61221 to North Ray crater material is found in the major and minor element chemistry of samples from these two sites. Table 1 gives the composition of these samples as reported previously (6). Soils from the North Ray crater site and sample 61221 have low nickel contents (109 to 176 parts per million). The low nickel content, low abundance of agglutinates, large grain size, and major and minor element chemistry of sample 61221 point to a very immature lunar soil, which is probably associated with

the North Ray crater event. In contrast, a comparison of the composition of the surface soil (61241) with those of subsurface sample 61221 and of samples collected from stations which are believed to lie on ray material from South Ray crater indicates that the upper material (61241) is probably derived from South Ray crater (Table 1). The relatively nickel-rich soils (316 to 363 ppm of nickel) from the ejecta blanket and rays of South Ray crater (including sample 61241) indicate that it could be the result of the impact of an iron-rich meteorite. Clearly, the mode of origin of North Ray crater was different from that of South Ray crater.

The total carbon analysis of sample 61221 gave 100 ± 10 ppm of carbon, whereas the darker mature soil 61241 overlying it contained 110 ± 10 ppm of carbon (6). Moore *et al.* (3) have postulated that the majority of the carbon found in lunar soils is derived from the solar wind. In this case, the high carbon content of soil 61221 is inconsistent with its immaturity or apparent lack of exposure to the solar wind. The anorthosite-rich rocks at the Apollo 16 site are extremely low in their carbon contents. Most of the rocks contain less than 6 ppm of total carbon (6). Sample 61221, although composed of mostly anorthositic components, typically with less than 6 ppm of carbon, is unusually rich in carbon. Thus, some special origin or genesis is required for this sample to explain its high carbon abundance.

Thermal analysis–gas release studies of 61221 provide further evidence of the unusual nature of this sample. The analyses were carried out by using a computer-controlled interfaced thermal analyzer–quadrupole mass spectrometer

Table 1. X-ray fluorescence analysis of Apollo 16 soils (6). Sample 61220,2 is the bulk sample from which 61221,11 was taken. Two samples were taken from North Ray crater and four samples from South Ray crater ejecta.

Component	61220,2 Station 1 subsurface white soil	Composition ranges of soil		61241,2 Station 1 surface soil
		North Ray crater	Stations 4, 5, 6 (South Ray crater ejecta)	
SiO$_2$ (%)	45.35	44.95– 45.28	44.88– 45.38	45.32
TiO$_2$ (%)	0.49	0.41– 0.42	0.55– 0.67	0.57
Al$_2$O$_3$ (%)	28.25	28.93– 29.01	26.22– 27.60	27.15
FeO (%)	4.55	4.09– 4.66	5.03– 6.08	5.33
MnO (%)	0.06	0.06	0.06– 0.08	0.07
MgO (%)	5.02	4.20– 4.75	5.35– 6.39	5.75
CaO (%)	16.21	16.40– 16.54	15.28– 15.81	15.69
Na$_2$O (%)	0.42	0.42– 0.44	0.38– 0.41	0.55
K$_2$O (%)	0.09	0.06– 0.07	0.10– 0.13	0.10
P$_2$O$_5$ (%)	0.10	0.06– 0.13	0.13– 0.15	0.13
S (%)	0.06	0.03– 0.04	0.07– 0.09	0.07
Sum (%)	100.6	100.4 –100.5	99.9 –100.6	100.7
		Trace elements		
Sr (ppm)	182	180–194	167–173	175
Ni (ppm)	109	111–176	316–362	320
Cr (ppm)	590	520–540	710–830	720
C (ppm)	100			110

system (8). Samples were heated at 6°C per minute from room temperature to 1000°C under a vacuum of 10^{-6} torr. The sample's weight loss, along with released gaseous species, abundances, temperature ranges, and sequences of release, were determined simultaneously during the heating cycle. The sensitivity of the analytical balance was ± 0.01 mg; hence, extremely small weight-loss changes could be observed.

Between 175° and 350°C, sample 61221 lost 0.03 percent by weight (approximately 300 ppm of volatiles). Figure 1 shows the weight-loss curve and gas release pattern. All lunar samples analyzed previously (approximately 30 from Apollo 11 through Apollo 16) show no measurable weight loss at temperatures below 800°C (8). The gas release profile of sample 61221 shows that the volatile components lost

between 175° and 350°C include H$_2$O, H$_2$, CO$_2$, HCN, and CH$_4$. Minor amounts of CO, N$_2$, and C$_2$H$_6$; hydrocarbon fragments of masses 39, 41, and 43; and possibly other volatile species were also present during this weight-loss step. A semiquantitative analysis showed the following relative concentrations of gases released during the weight-loss step (percent by weight): H$_2$O (40–50), CO$_2$ (15–20), H$_2$ (5–10), HCN (5–10), CH$_4$ (5–10), CO or N$_2$, or both (2–5), and hydrocarbons (1–5). The volatiles released in the interval 175° to 350°C are distinctly different in their release profiles from terrestrially adsorbed species and gases derived from the solar wind (8). The abundance of hydrogen derived from the solar wind (H$_2$ released between 300° and 700°C) (Fig. 1) is much lower for soil 61221 than the amount of H$_2$ found in more mature lunar soils (8). This is further evidence of the short surface residence time of soil sample 61221. The quantity of CO$_2$ released in the weight-loss region is considerably greater than for any previously analyzed lunar sample which we have seen. Hayes (9) noted that the normal CO/CO$_2$ ratio for mature lunar soils is approximately 6 to 8, whereas sample 61221 has a ratio of 2 to 3. The lower ratio suggests that 61221 was subjected to a more oxidizing environment than were previously examined lunar samples, except possibly the Apollo 16 rocks which contain the goethite (6).

The low-temperature profiles for release of water and hydrogen from soil 61221 (Fig. 1) are unique for lunar samples. Determinations of the H/D ratio of these gases along with the ^{12}C/^{13}C ratio of the CO$_2$ of the low-temperature volatiles will be important in establishing whether these components are of terrestrial or extraterrestrial origin.

The precise source of the volatile components in 61221 is presently unknown. Contamination of the sample during collection, return, and subsequent processing and handling seems unlikely because of the absence of loosely adsorbed contaminants (H$_2$O, N$_2$, and CO$_2$ released below 150°C) and the fact that the sample was returned to Earth in an Apollo Lunar Sample Return Container (ALSRC). The low-temperature volatiles are not typical of those associated with carbonaceous chondrite type materials (8). Sulfur-containing species (SO$_2$, H$_2$S, CS$_2$) are generally released from car-
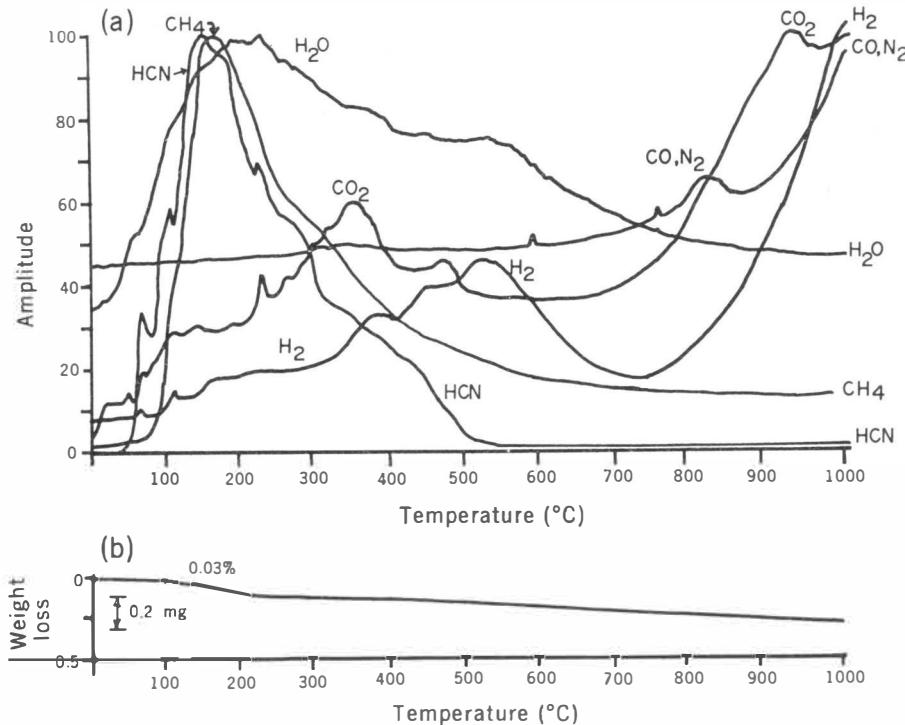

Fig. 1. (a) Gas release pattern and (b) weight-loss curve for Apollo 16 subsurface soil 61221,11. The sample, which weighed 320 mg, was heated at 6°C per minute to 1000°C; the total weight loss was 0.07 percent. The patterns of gas release have been plotted so that each gas is normalized to 100 percent amplitude in its region of greatest abundance.

bonaceous chondrite material around 400° to 600°C. Sample 61221 did not evolve any sulfur-containing gases until temperatures above 900°C, and these high-temperature sulfur gases are reaction products of sulfur-bearing phases found in the soils with the silicate phases (8).

If the soil 61221 is associated with North Ray crater, as suggested by morphological and chemical characteristics, we suggest that the volatile material may have been brought to this site by the object that formed North Ray crater. Whipple (10) and Wurm (11) noted that the neutral molecules CN, C_2, C_3, NH, CH, OH, and NH_2, along with the ionized molecules CO^+, N_2^+, CH^+, CO_2^+, and OH^+, are characteristic components of comets. The possible parent compounds (H_2O, CO_2, HCN, H_2, CO, CH_4, N_2) of all these cometary species have been identified in lunar soil 61221. The large abundance of HCN in soil 61221, as compared to other lunar soils, is particularly strong evidence for this hypothesis. Hydrogen cyanide and hydrocarbon fragments have been previously identified in lunar soils and as exhaust products of the lunar module (LM) (12), but their abundance and temperature release profiles are distinctly different from the pattern observed for sample 61221. The subsurface location of sample 61221 further reduces the possibility of LM exhaust contamination. Kopal (13) points out that the total amount of gas which can be acquired by the moon in a catastrophic encounter with a comet is far from negligible. Although the exact composition of the gases associated with a cold cometary nucleus is not known at the present time, those gases identified in the spectra of cometary tails provide us with evidence of possible constituents that might be derived from a comet during impact.

If North Ray crater was formed by a cometary impact, it is possible that portions of the volatiles in the comet were retained in ray material thrown out as a result of the impact. Had the impact occurred during the cold lunar night the retention of volatiles would have been even more efficient. If the Apollo 15 heat flow measurements can be extrapolated to the Apollo 16 site (14), that part of the crater ray at a depth of 30 to 35 cm would have had a mean temperature of approximately 0°C after it cooled. Further burial would result from the base surge deposits emanating from younger craters, such as South Ray crater and secondary craters in the area immediately surrounding Plum crater. The probability of the retention of gases and volatiles from the comet after impact is quite low, but rapid burial might allow a small portion of them to be preserved. The presence of HCN, the low-temperature release of CH_4, and the unique weight-loss profile of sample 61221 suggest that it may have formed in the manner outlined. Studies of the abundances of such volatile elements as bismuth, lead, and thallium in sample 61221 may further test the proposed unique origin of this volatile-rich lunar soil.

EVERETT K. GIBSON, JR.
TN7 Geochemistry Branch,
NASA Manned Spacecraft Center,
Houston, Texas 77058

GARY W. MOORE
Lockheed Electronics Corporation,
Houston, Texas 77058

References and Notes

1. "The Moon Issue," *Science* **167** (1970); "Proceedings of the Apollo 11 Lunar Science Conference," *Geochim. Cosmochim. Acta* **1–3** (Suppl. 1) (1970).
2. E. Anders, *Science* **169**, 1309 (1970).
3. C. B. Moore, E. K. Gibson, Jr., J. W. Larimer, C. F. Lewis, W. Nichiporuk, *Geochim. Cosmochim. Acta* **2** (Suppl. 1), 1375 (1970).
4. C. Duke, personal communication; Apollo Lunar Geology Investigation Team, *Astrogeology 51* (Interagency report, U.S. Geological Survey, Washington, D.C., 1972).
6. Apollo 16 Preliminary Examination Team, *Science* **179**, 23 (1973).
7. D. S. McKay, D. A. Morrison, U. S. Clanton, G. H. Ladle, J. F. Lindsay, *Geochim. Cosmochim. Acta* **1** (Suppl. 2), 755 (1971); D. S. McKay, G. H. Heiken, R. M. Taylor, J. S. Clanton, D. A. Morrison, *ibid.*, in press; U. S. Clanton, D. S. McKay, R. M. Taylor, H. Heiken, *The Apollo 15 Samples* (Lunar Science Institute, Houston, Texas, 1972).
8. E. K. Gibson, Jr., and S. M. Johnson, *Geochim. Cosmochim. Acta* **2** (Suppl. 2), 1351 (1971); E. K. Gibson, Jr., and G. W. Moore, *ibid.*, in press; E. K. Gibson, Jr., and S. M. Johnson, *Thermochim. Acta* **4**, 49 (1972); E. K. Gibson, Jr., *ibid.*, in press.
9. J. Hayes, personal communication.
10. F. J. Whipple, in *The Moon, Meteorites and Comets*, B. M. Middlehurst and G. P. Kuiper, Eds. (Univ. of Chicago Press, Chicago, 1963), pp. 639–664.
11. K. Wurm, in *ibid.*, pp. 573–617.
12. B. R. Simoneit, A. L. Burlingame, D. A. Flory, I. D. Smith, *Science* **166**, 733 (1969); P. T. Holland, B. R. Simoneit, P. C. Wszolek, W. H. McFadden, A. L. Burlingame, *Geochim. Cosmochim. Acta*, in press; D. A. Flory, S. Wikstrom, S. Gupta, J. M. Gibert, J. Oró, *ibid.*, in press.
13. Z. Kopal, *Man and His Universe* (Morrow, New York, 1972), pp. 182–188.
14. M. G. Langseth, Jr., S. P. Clark, Jr., J. L. Chute, Jr., S. J. Keihm, A. E. Wechsler, *Apollo 15 Preliminary Science Report* (NASA SP-289, National Aeronautics and Space Administration, Washington, D.C., 1972), p. 11-1.
15. We thank J. Hayes for confirming our suspicion as to the unusual nature of sample 61221. The authors acknowledge the invaluable assistance of astronaut C. Duke and discussions with P. W. Gast, P. R. Brett, S. Chang, D. S. McKay, G. H. Heiken, D. A. Flory, K. Kvenvolden, and C. B. Moore.

15 September 1972; revised 30 October 1972